Journal of Medicinal Chemistry Article

J. Med. Chem. **2009,** *52,* 5649–5661 **5649**
DOI: 10.1021/jm900469e

Discovery of a Novel Series of Quinolone and Naphthyridine Derivatives as Potential Topoisomerase I Inhibitors by Scaffold Modification

Qi-Dong You,*[,†] Zhi-Yu Li,[†] Chiung-Hua Huang,[§] Qian Yang,[†] Xiao-Jian Wang,[†] Qing-Long Guo,[†] Xiao-Guang Chen,[‡] Xun-Gui He,[†] Tsai-Kun Li,[∥] and Ji-Wang Chern*[,§,⊥]

[†]*School of Pharmacy, China Pharmaceutical University, Nanjing 210009, China,* [‡]*Institute of Materia Medica, Chinese Academy of Medical Sciences & Peking Union Medical College, Beijing 100050, China,* [§]*School of Pharmacy and* [∥]*Department of Microbiology, College of Medicine and* [⊥]*Department of Life Science, College of Life Science, National Taiwan University, No. 1, Section 1, Ren-Ai Road, Taipei 100, Taiwan*

Received March 17, 2009

A novel series of topoisomerase I (Top I) inhibitors were designed on the basis of camptothecin using scaffold modification strategy. Thirty-one new compounds were synthesized and evaluated for anticell proliferation activity. The most potent compound **26** presented a significant inhibitory effect on Top I, leading to Top I-mediated cleavage and influences on Top I expression at the cellular level. Moreover, **26** was proved to induce cell death via apoptosis and accelerated DNA strand breaks without significant alteration in cell cycle populations. All of the experimental results herein indicated that **26** could interact with DNA−Top I complex and induce cancer cell apoptosis to produce antitumor effects. The *in vivo* evaluation of **26** on the growth of HT-29 tumor xenografts in nude mice suggested its therapeutic potential for further development.

Introduction

DNA topoisomerase I (Top I)[a] is ubiquitous and essential in mammals, and this enzyme is involved in tumor growth. Traditional Top I inhibitors, like the natural pentacyclic alkaloid camptothecin (CPT, **1**),[1,2] can bind and stabilize a binary DNA−Top I complex containing a single-strand nick,[3,4] thus inhibiting DNA replication and eventually causing cell death during the S phase of the cell cycle. This unique mechanism of action coupled with the initial success of **1** in preclinical studies provoked a flurry of research on this important natural compound in the hope of developing a novel anticancer drug for managing human malignancies. Unfortunately, clinical applications of **1** have been thwarted by the compound's high toxicity and poor water solubility. Therefore, tremendous efforts have been made to develop semisynthetic and more water-soluble analogues of **1**, such as topotecan (TPT, **3**) and irinotecan (**4**), which are derivatives of 10-hydroxycamptothecin (HCPT, **2**) and have been approved for clinical treatment of cancer patients.[5,6] However, the therapeutic potential of **1** and its derivatives is severely hindered due to their rapid inactivation through lactone ring hydrolysis at physiological pH (Scheme 1).[7] Considering that Top I is a proven and effective target for cancer treatment, metabolically stable non-CPT derivatives have been developed,[8−11] like indolocarbazoles and indenoisoquinolines, some of which are now in clinical evaluation. In view of the successful clinical cases of these non-CPT derivatives, it was reasoned that the better chemical stability at longer lifetimes of the trapped cleavage complex of the non-CPT Top I inhibitors was due to the absence of a lactone ring in their skeleton.[12] The scaffold modification approach has been generally accepted as a means to transform one pharmacophoric template into another.[13] The rationale behind this type of transformation is that the new template will retain some of the characteristics of the original template but exhibit improved potency, selectivity, and pharmacokinetics. Consequently, we attempted to synthesize compounds lacking the lactone ring of **1** and change the rigid framework of **1** into a combination of the quinolone skeleton and benzimidazole group or its bioisoesters having a single carbon bond (Figure 1A). The target scaffold depicted in Figure 1B possesses an identical arrangement and similar distance of every H-bond donors and acceptors when compared with **1**. We reasoned that the fluoro atom and piperazine on the skeleton could be the scaffold to enhance the druglike properties: To our best knowledge, the fluoro atom could improve the metabolic characteristics of compounds by prolonging the half-lives, and the piperazine could enhance the water solubility of compounds. Herein, we present the synthesis and biological studies of a series of 3-substituted quinoline and naphthyridine compounds as potential anticancer agents by inhibiting Top I.

*To whom correspondence should be addressed. (Q.-D.Y.) Phone: +86-25-83271351. Fax: +86-25-83271351. E-mail: youqidong@gmail.com. (J.-W.C.) Phone: +886-2-2393-9462. Fax: +886-2-2393-4221. E-mail: jwchern@ntu.edu.tw.

[a] Abbreviations: CPT, camptothecin; EGFP, enhanced green fluorescent protein; HCPT, 10-hydroxycamptothecin; MTT; 1-*N*-methyl-5-thiotetrazole; PI, propidium iodide; PPA, polyphosphoric acid; SRB, sulforhodamine B; SSGE, single-cell gel electrophoresis; Top I, topoisomerase I; TPT, topotecan.

Results and Discussion

Chemistry. The targets **6**−**36** (Table 1) were synthesized as outlined in Scheme 2. Quinolone-3-carboxylic acids or naphthyridine-3-carboxylic acids were condensed with *o*-phenylenediamine, *o*-aminophenol, or *o*-aminobenzenethiol in polyphosphoric acid (PPA) at 170−250 °C to obtain **6**−**20**.

Published on Web 08/28/2009

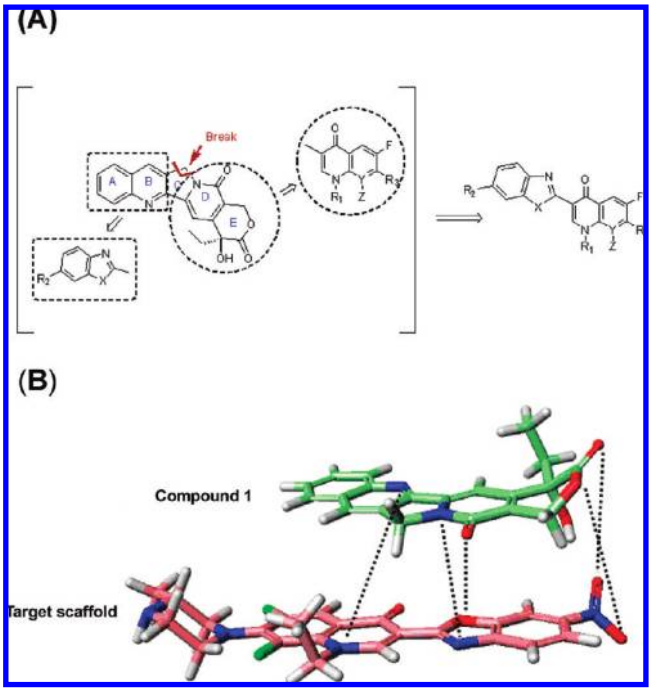

Figure 1. Compound generation by scaffold modification. (A) Scaffold designed based on **1**. (B) Superimposition of target scaffold with **1**.

Scheme 1. Structures of **1** Derivatives[a]

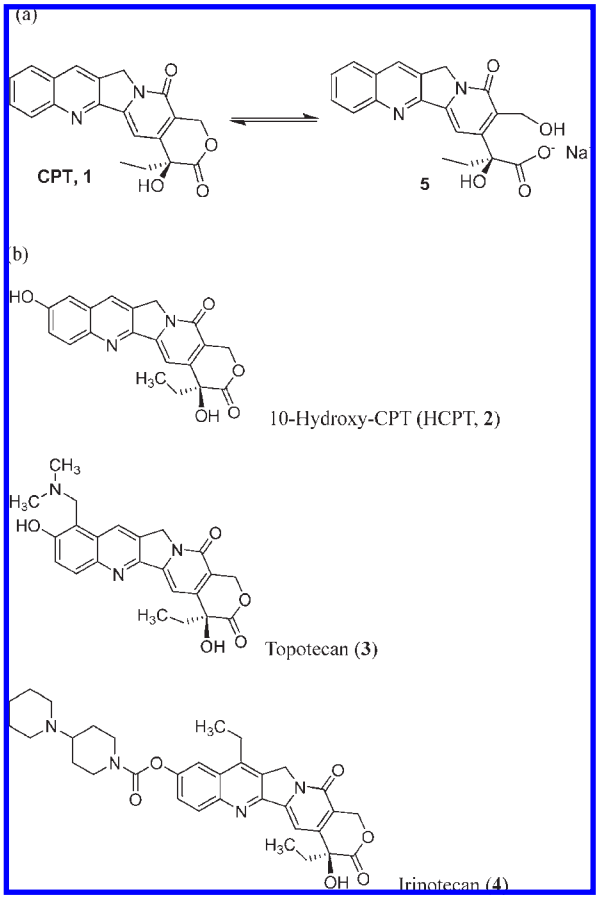

[a] (a) Lactone ring hydrolysis of **1**. (b) Clinically approved **1** derivatives.

Subsequently, **6**−**18** were subjected to nitration in a mixture of concentrated H_2SO_4 and HNO_3 (1:1.2−1.3) at 5 °C and then heated for 1−2 h at 40−45 °C to afford **21**−**33**. Compounds **21**, **22**, and **24** were subjected to hydrogen reduction with Pd/C to give **34**−**36**.

Cytotoxicity of Quinolone and Naphthyridine Derivatives in Various Human Cancer Cell Lines. Compound **1** derivatives, which selectively target DNA−Top I, are among the most effective anticancer drugs (especially against solid tumors) recently approved by the U.S. Food and Drug Administration. We used the 1-*N*-methyl-5-thiotetrazole (MTT)-based assay to evaluate the antiproliferative effect of quinolone and naphthyridine derivatives **6**−**36** in three cancer cell lines. Table 1 lists cytotoxic activities of two main skeleton quinoline and naphthyridine derivatives containing three kinds of heterocycles, such as benzimidazole, benzoxazole, and benzothiazole at the 3-position. Certain compounds demonstrated cytotoxicity comparable to **2**. By comparing the basic skeletons of these three heterocycles in **6**−**18**, the most active structural feature relevant to cytotoxicity against the three tumor cell lines appeared to be the 3-benzothiazole-naphthyridine skeleton **15** with an IC_{50} in the 2.4−2.7 μM range. In general, the piperidinyl side chain at the 7-position yielded greater cytotoxicity than compounds containing the 3-methyl- or 4-methyl-piperidinyl side chains. Interestingly, **20**, containing a naphthyridine nucleus and a piperidinyl side chain with a chlorine atom at the 6-position of benzimidazole, was more cytotoxic than **19**, which contains a quinolone nucleus. We presumed that an electron-withdrawing group at the 6-position of the benzimidazole ring may contribute to the cytotoxicity. Thus, a series of **21**−**33** with a nitro group at the 6-position of the benzimidazole, benzoxazole, and benzothiazole rings was synthesized and evaluated. Most of these compounds, except for **22**, **27**, and **30**, exhibited better cytotoxicity (IC_{50} range, 0.2−7.7 μM) than **6**−**18**. Among **21**−**33**, **26**, a quinolone nucleus with a 3-benzoxazole substituent, had an IC_{50} range of 0.2−0.6 μM, better than the other compounds containing a 3-benzimidazole or 3-benzothiazole ring. Interestingly, **34** and **35**, obtained by further reduction of the nitro group of **21** and **24**, had dramatically reduced cytotoxicity, lending support to the presumption that an electron-withdrawing group at position 6 may be important for cytotoxicity. Notably, a methyl group on the piperidine substituent in **6**−**18** reduced cytotoxicity. However, this phenomenon was not observed in the nitro-compound series **21**−**33**. Table 1 shows that **6**, **7**, **20**, **23**, **26**, **28**, and **31**−**36** showed potential cytotoxicity with IC_{50} values in the submicromolar range, and thus, we further evaluated the cytotoxicity of these compounds against 12 human cancer cell lines using a colorimetric sulforhodamine B (SRB) protein dye staining method or MTT assay. On the basis of Table 2, **26** showed the greatest potential cytotoxicity with an IC_{50} range of 0.7−5.5 μM, and long-term treatment (14 days) of HT-29 human colorectal adenocarcinoma cells with 5 μM 26 almost completely inhibited anchorage-dependent colony formation (Figure 2).

Effect of Quinolone and Naphthyridine Derivatives on Top I Activity. In principle, inhibitors of DNA topoisomerases could act at any of the three major steps comprising the enzyme reaction mechanism, namely, enzyme binding to DNA, cleavage of DNA strands, and religation of the DNA following the strand-passing step.[10] To investigate the mechanism(s) by which our synthetic compounds inhibited Top I and thereby caused cytotoxicity, the effect of quinolone and naphthyridine derivatives on Top I activity was examined by measuring the relaxation of supercoiled

Table 1. Structure and in Vitro MTT Assay Results for Quinolone and Naphthyridine Derivatives

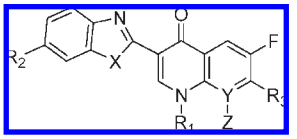

compound no.	structure						cytotoxicity (IC_{50}, μM)[a]		
	X	Y	Z	R_1	R_2	R_3	KB	A2780	Bel7402
2							0.6 ± 0.1	0.7 ± 0.1	0.2 ± 0.1
6	NH	C	H	Et	H	piperazin-1-yl	10.5 ± 2.0	0.8 ± 0.3	27.4 ± 5.1
7	NH	N		Et	H	piperazin-1-yl	2.0 ± 0.3	4.8 ± 1.0	4.1 ± 0.3
8	NH	C	F	Et	H	3-methylpiperazin-1-yl	19.1 ± 4.0	11.6 ± 0.9	30.2 ± 3.5
9	NH	C	H	Et	H	4-methylpiperazin-1-yl	36.7 ± 7.8	> 5018.2 ± 2.7	
10	O	C	H	Et	H	chlorine	10.2 ± 1.5	78.4 ± 8.8	28.9 ± 3.2
11	O	C	F	Et	H	3-methylpiperazin-1-yl	18.9 ± 2.8	83.5 ± 11.8	5.7 ± 1.4
12	O	C	H	Et	H	4-methylpiperazin-1-yl	87.4 ± 11.3	0.7 ± 0.2	2.0 ± 0.2
13	O	N		Et	H	piperazin-1-yl	11.7 ± 2.3	15.3 ± 1.3	16.8 ± 2.0
14	S	C	H	Et	H	piperazin-1-yl	28.7 ± 3.2	11.3 ± 0.5	24.3 ± 3.0
15	S	N		Et	H	piperazin-1-yl	2.4 ± 0.2	2.7 ± 0.2	2.4 ± 0.7
16	S	C	H	Et	H	4-methylpiperazin-1-yl	19.0 ± 2.1	114.0 ± 16.6	24.0 ± 4.7
17	S	C	(S)−CH $(CH_3)CH_2O$−		H	4-methylpiperazin-1-yl	60.2 ± 11.1	26.6 ± 2.2	92.2 ± 21.1
18	S	C	F	Et	H	3-methylpiperazin-1-yl	24.3 ± 2.7	9.8 ± 1.4	15.0 ± 2.0
19	NH	N		Et	Cl	piperazin-1-yl	10.3 ± 1.2	6.3 ± 0.7	21.5 ± 3.3
20	NH	C	H	Et	Cl	piperazin-1-yl	1.6 ± 0.2	4.9 ± 0.5	2.8 ± 0.5
21	NH	C	H	Et	NO_2	piperazin-1-yl	1.1 ± 0.2	1.6 ± 0.2	2.1 ± 0.7
22	NH	N		Et	NO_2	piperazin-1-yl	22.4 ± 2.7	12.4 ± 1.8	10.8 ± 1.8
23	NH	C	F	Et	NO_2	3-methylpiperazin-1-yl	2.3 ± 0.2	2.3 ± 0.4	1.1 ± 0.2
24	NH	C	H	Et	NO_2	4-methylpiperazin-1-yl	2.5 ± 1.0	4.7 ± 0.7	4.4 ± 0.9
25	O	C	H	Et	NO_2	chlorine	0.5 ± 0.3	ND[b]	1.8 ± 0.3
26	O	C	F	Et	NO_2	3-methylpiperazin-1-yl	0.6 ± 0.2	0.2 ± 0.2	0.2 ± 0.2
27	O	C	H	Et	NO_2	4-methylpiperazin-1-yl	40.3 ± 13.0	39.6 ± 8.6	50.2 ± 6.6
28	O	N		Et	NO_2	piperazin-1-yl	1.8 ± 0.2	ND[b]	3.0 ± 0.5
29	S	C	H	Et	NO_2	piperazin-1-yl	0.7 ± 0.2	0.7 ± 0.2	1.8 ± 0.2
30	S	N		Et	NO_2	piperazin-1-yl	179.3 ± 22.2	200.2 ± 33.0	24.6 ± 6.6
31	S	C	H	Et	NO_2	4-methylpiperazin-1-yl	5.8 ± 1.0	4.3 ± 1.3	7.7 ± 1.3
32	S	C	(S)−CH $(CH_3)CH_2O$−		NO_2	4-methylpiperazin-1-yl	0.6 ± 0.2	1.2 ± 0.2	2.0 ± 0.4
33	S	C	F	Et	NO_2	3-methylpiperazin-1-yl	4.7 ± 1.2	3.3 ± 1.2	4.1 ± 0.8
34	NH	C	H	Et	NH_2	piperazin-1-yl	35.4 ± 5.2	51.5 ± 8.7	92.1 ± 11.6
35	NH	C	H	Et	NH_2	4-methylpiperazin-1-yl	> 50	> 50	> 50
36	NH	N		Et	NH_2	piperazin-1-yl	30.1 ± 4.1	42.3 ± 7.2	93.3 ± 13.9

[a] The cytotoxicity IC_{50} values are the concentrations corresponding to 50% cell death. [b] ND, not determined; KB, oral epidermal carcinoma cell line; A2780, ovarian carcinoma cell line; and Bel-7402, hepatocellular carcinoma cells.

Scheme 2. Synthesis of Quinolone and Naphthyridine Derivatives[a]

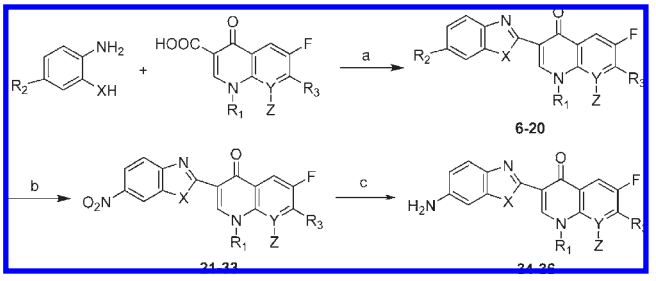

[a] Reagents and conditions: (a) PPA, N_2, 170−250 °C. (b) HNO_3, H_2SO_4, 40−45 °C. (c) Pd/C.

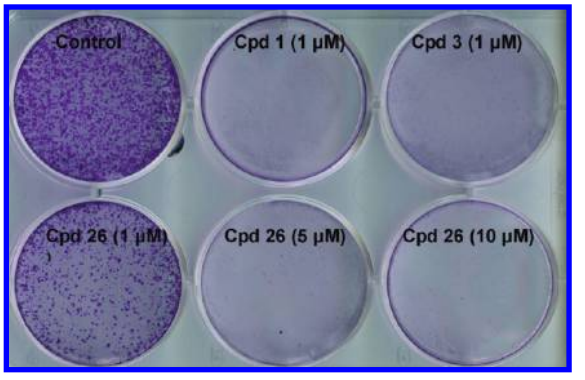

Figure 2. Long-term inhibitory effect of **26** showing inhibition of anchorage-dependent colony formation. Cpd **1**, CPT; Cpd **3**, TPT; and Cpd **26**, compound **26**.

DNA of plasmid pBR322. We also compared the inhibitory activities of these series of derivatives with a known DNA−Top I inhibitor, **1** (Figure 3). Although the inhibition at the higher **1** concentrations (100−1000 μM) was abundant, the products were more heterogeneous as compared with those observed at lower **1** concentrations (Figure 3A,B). Top I inhibition was similar for **1** and

Table 2. In Vitro SRB Assay To Test the Effectiveness of 12 Quinolone and Naphthyridine Derivatives against 12 Cancer Cell Lines[a]

cell line	HeLa		HT-29		AGS		MCF-7		MDA-MB-261		A549		HepG2		Hep3B		PC-3		U937	THP-1	K562
p53 status	null[b]		mt[c]		wt[d]		wt (ER+)[e]		mt (ER−)[f]		wt		wt		null		null		mt	mt	null
compds (μM)	GI_{50}	IC_{50}	GI_{50}	IC_{50}	GI_{50}	IC_{50}	GI_{50}	IC_{50}	GI_{50}	IC_{50}	GI_{50}	IC_{50}	GI_{50}	IC_{50}	GI_{50}	IC_{50}	GI_{50}	IC_{50}	IC_{50}	IC_{50}	IC_{50}
1	0.04	0.2	0.03	0.4	0.01	0.02	0.01	1.1	0.08	1.7	0.01	0.04	0.1	0.2	0.01	0.06	0.7	1.4	0.3	0.6	1.4
3	0.08	1.6	0.08	0.4	0.1	0.3	0.8	2.0	0.9	2.0	0.9	1.9	1.2	1.6	0.4	1.4	1.3	2.0	1.1	1.5	1.7
6	>10	>10	>10	>10	9.5	>10	>10	>10	>10	>10	0.6	4.7	>10	>10	>10	>10	>10	>10	>10	>10	>10
7	6.4	10	>10	>10	2.1	6.6	8.3	9.5	3.3	10	4.9	7.8	6.8	9.1	3.7	7.8	>10	>10	>10	>10	9.1
20	1.2	4.2	1.8	4.7	4.5	1.0	4.2	4.5	0.9	2.3	1.0	0.5	1.8	3.7	0.9	2.3	3.3	4.8	4.2	2.8	2.7
23	1.4	2.4	4.2	7.5	2.6	8.2	2.6	4.9	1.8	5.5	0.6	2.4	1.5	4.2	1.6	5.5	7.9	9.6	>10	7.8	4.7
26	1.1	2.4	1.0	5.5	0.7	3.5	3.0	6.8	0.7	3.1	0.8	1.5	2.8	4.5	1.5	3.9	3.3	4.2	1.4	3.5	4.6
28	>10	>10	>10	>10	2.3	4.4	>10	>10	>10	>10	2.1	7.3	>10	>10	>10	>10	5.8	9.8	>10	>10	>10
31	>10	>10	>10	>10	2.6	4.5	>10	>10	>10	>10	4.7	10	>10	>10	>10	>10	5.5	7.5	>10	>10	>10
32	>10	>10	5.0	10	7.0	8.8	>10	>10	>10	>10	3.9	>10	7.6	>10	>10	>10	1.8	9.9	>10	>10	>10
33	1.7	9.9	1.0	5.0	3.3	5.4	>10	>10	2.3	7.4	1.5	7.0	0.9	3.6	0.6	1.4	2.7	10	>10	>10	>10
34	>10	>10	>10	>10	7.8	10	>10	>10	>10	>10	>10	>10	>10	>10	>10	>10	>10	>10	>10	10	>10
35	>10	>10	>10	>10	10	>10	>10	>10	>10	>10	1.0	>10	>10	>10	>10	>10	>10	>10	>10	>10	>10
36	>10	>10	>10	>10	6.7	9.2	>10	>10	>10	>10	0.5	>10	>10	>10	>10	>10	>10	>10	>10	8.2	>10

[a] HeLa, cervical adenocarcinoma; HT-29, colorectal adenocarcinoma; AGS, gastric adenocarcinoma; MCF-7 and MDA-MB-261, breast adenocarcinoma; A549, lung carcinoma; HepG2 and Hep3B, hepatocarcinoma; PC-3, prostate adenocarcinoma; THP-1, acute monocytic leukemia cells; K562, chronic myelogenous leukemia cells; and U937, acute myeloid leukemia cells. Titrated concentrations of test compounds: 10, 5, 2.5, 1.25, 0.63, 0.32, 0.15, 0.08, and 0 μM. Titrated concentrations of **1** and **3**: 2, 1, 0.5, 0.25, 0.125, 0.063, 0.032, 0.015, and 0 μM. [b] Null, no expression. [c] mt, mutant type. [d] wt, wild type. [e] ER(+), estrogen receptor positive. [f] ER(−), estrogen receptor negative.

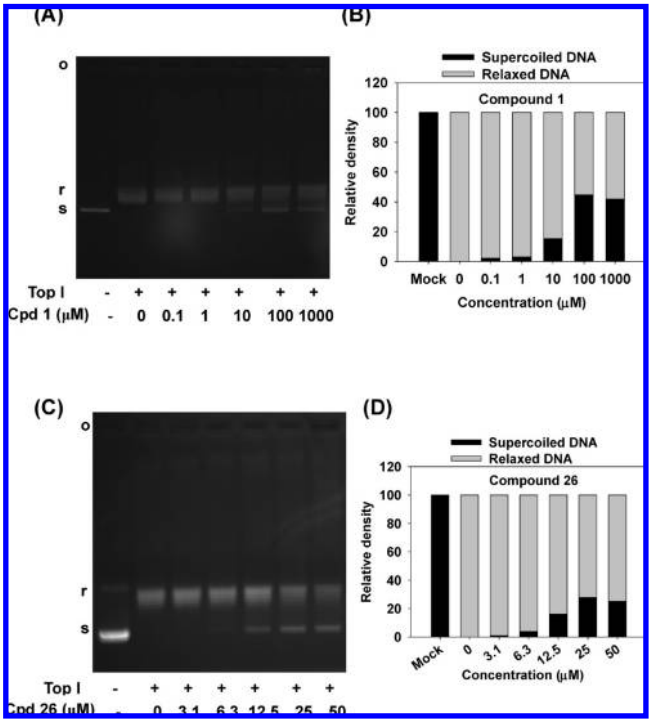

Figure 3. Effects of **1** and **26** on Top I-mediated DNA relaxation. (A, C) The position of the origin (o) and the migration positions of relaxed (r) and supercoiled (s) plasmids are shown on the left. (B, D) Dose responses for the effects of **1** and **26**, respectively, on Top I-mediated DNA relaxation. The proportion of relaxed DNA to total DNA was measured by scanning with an imaging system. Bars show the percentage of supercoiled vs relaxed DNA.

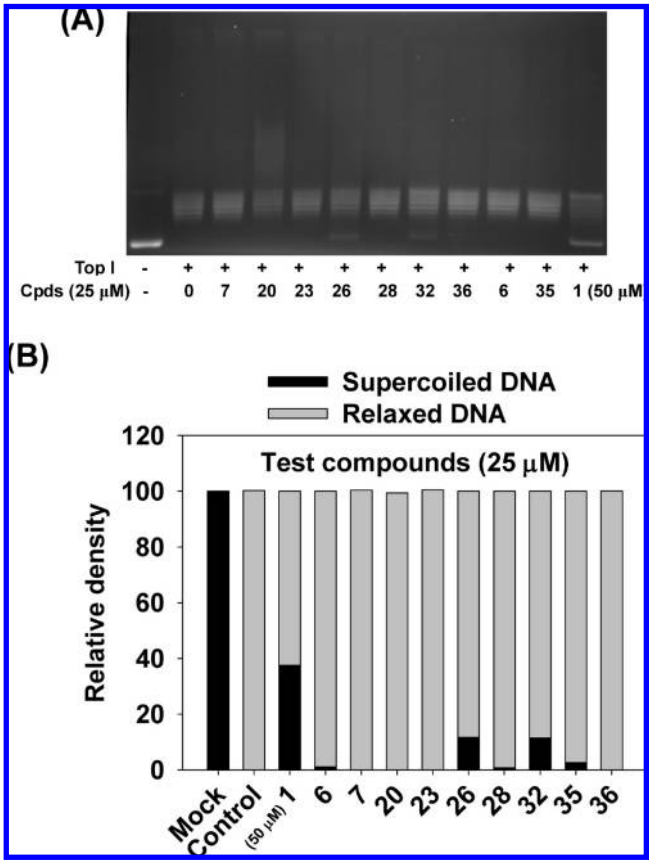

Figure 4. Effects of quinolone and naphthyridine derivatives on Top I-mediated DNA relaxation activity. (A) Lane 1, supercoiled pBR322 DNA; and lane 2, with Top I but no test compounds (Cpds). (B) Effects of test compounds on Top I-mediated DNA relaxation. The proportion of relaxed DNA to total DNA was measured by scanning with an imaging system. Bars show the percentage of supercoiled vs relaxed DNA.

26 at lower concentrations up to 12.5 μM of **26** (Figure 3C, D), but **1** was a much stronger inhibitor at higher concentrations.

In parallel, we tested our other compounds for Top I inhibition (Figure 4A,B). Despite moderate inhibition of **26** and **32** on Top I at 25 μM, most of the test compounds did not appreciably inhibit the enzyme at this concentration. However, because of the poor solubility of these compounds, at higher concentrations of 50 μM, these compounds were precipitated out under typical assay conditions.

Prompted by the above results, **26** was further investigated for the influence of Top I protein expression by immuno-

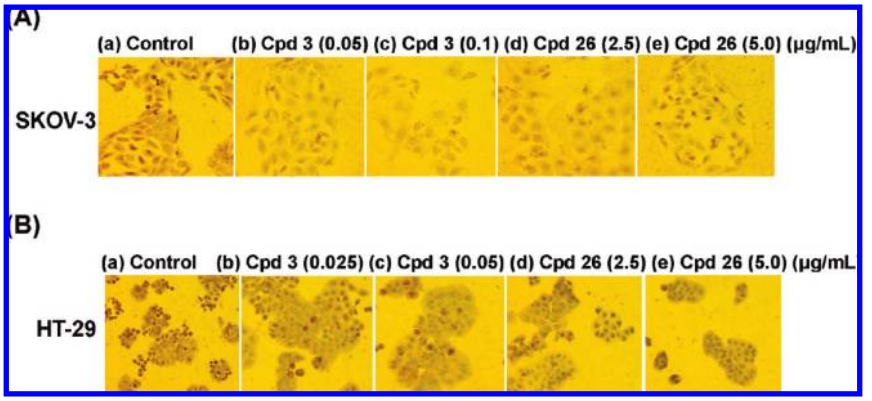

Figure 5. Effects of **26** on Top I expression in SKOV-3 and HT-29 cells. Cells were grown on microscope slides, fixed, permeabilized, and double-stained with Top I antibodies. Compound **26** was included at the concentrations indicated. Control, no compound added.

cytochemistry.[14] Cancer cell lines HT-29 and human ovarian cancer cells SKOV-3 were selected because **26** strongly inhibited the proliferation (for HT-29 cells, the IC_{50} value is 0.37 μg/mL; for SKOV-3 cells, the IC_{50} value is 0.55 μg/mL) in the MTT assay. As shown in Figure 5, Top I protein expression in HT-29 and SKOV-3 cells treated with **26** was significantly lower than in control cells, and the effect was dose-dependent, suggesting that **26** is able to both directly inhibit Top I and lower Top I protein expression at the cellular level.

Effect of 26 on Top I-Mediated Cleavable Complexes. Further studies of DNA cleavage in Top I were then performed in the presence of purified recombinant human Top I and a 3k base pair radiolabeled DNA. The extent of DNA fragmentation that occurs in the presence of Top I and various concentrations of **26** and **1** is shown in Figure 6A and quantitated in Figure 6B. Compounds **1** and **26** have Top I-targeting cleavage activity, as revealed by agarose gel electrophoresis of alkali-denatured ^{32}P-labeled linearized pRYG plasmid DNA. The potency of Top I-mediated cleavage activities of **26** was less than **1**; however, the cleavage pattern induced by **26** was not identical to that of **1**, which indicated that the **26** consensus sequence was different from that of **1**. These results suggested that **26** at pharmacologically relevant doses was primarily Top I poisons with DNA cleavage patterns exhibiting differences from **1**.

Effect of 26 on DNA Distribution in HT-29 Cells. Previous studies in rapidly proliferating cells suggested that the cytotoxicity of the DNA−Top I inhibitor, **1**, depends on active DNA replication.[15] Thus, the effects of **1** and **3**, and **26** at 1, 5, and 10 μM for 6, 12, 24, and 48 h on the percentage of HT-29 cells in each phase of the cell cycle were evaluated via flow cytometry. As shown in representative histograms presented in Figure 7A−D, short-term (6, 12, and 24 h) and a low dose (0.1 μM) of the Top I inhibitors **1** and **3** caused an increase in the percentage of HT-29 cells in the S phase because of diminished DNA synthesis. Prolonged exposure up to 48 h resulted in an overall increase in the number of cells in the S and sub-G1 phases, suggesting that **1** and **3** are highly effective to HT-29 cells, shifting the cell cycle distribution to the early S phase followed by induction of apoptosis. Interestingly, **26**-induced cytotoxicity did not coincide with a significant alteration in cell cycle populations, as only 5% of treated (up to 10 μM) cells were in the S phase, which was similar to control (Figure 7E). To quantify the degree of apoptosis, cells in the sub-G1 peak were counted and

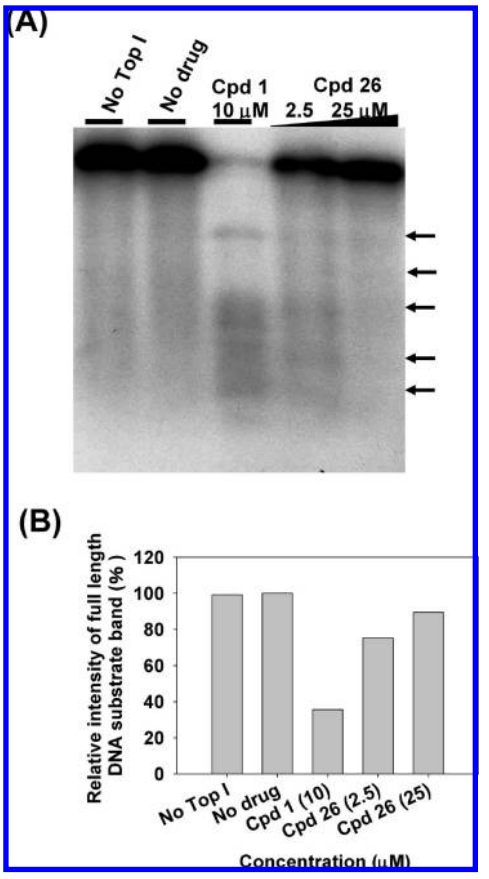

Figure 6. Stimulation of Top I-mediated DNA cleavage by compound **26**. (A) A representative agarose gel from Top I-mediated DNA cleavage carried out in the presence of positive compound **1** and compound **26**. (B) Quantitative determination of the relative intensity of the full length DNA substrate band using an imaging system.

expressed as a percentage of the total cell population (Figure 7F). Remarkably, only about 4.4% of the control cells were in the apoptotic peak at 48 h, whereas 0.1 μM **1**, 0.1 μM **3**, and 1 μM **26** increased the number of apoptotic cells to 44.8, 40.5, and 35.5%, respectively. Compound **26** potently reduced the number of HT-29 cells with diploid DNA content (G0/G1 region) as compared with control, and it caused a corresponding increase in the number of cells with hypodiploid DNA content (sub-G1 region), indicative of apoptosis and necrosis. These cytotoxicity results indicated

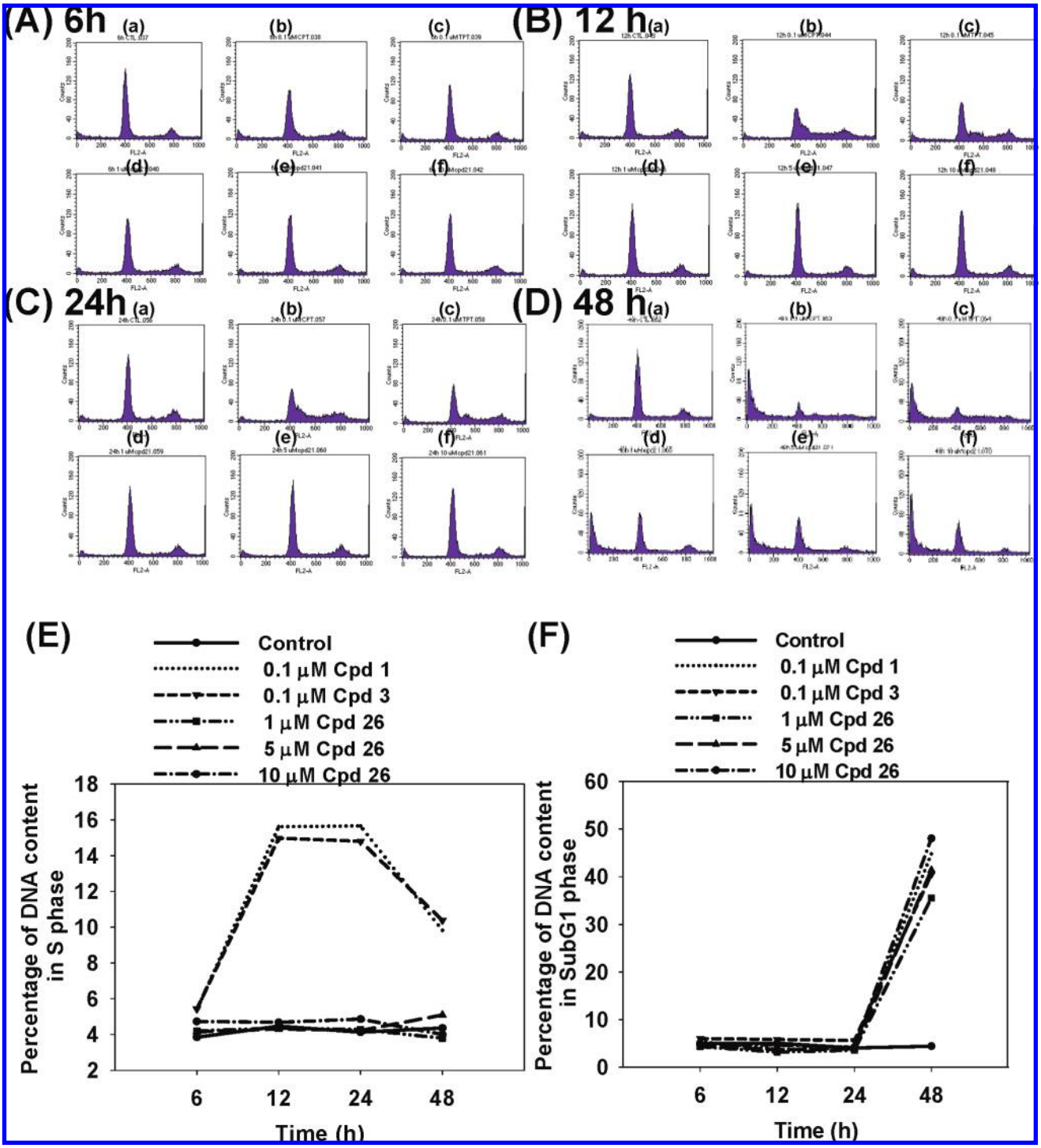

Figure 7. Quantification of cell cycle distribution of HT-29 cells by flow cytometry. (A−D) DNA histograms of HT-29 cells at the indicated time points after the addition of **26**. (a) Control, (b) **1** (0.1 μM), (c) **3** (0.1 μM), (d) **26** (1 μM), (e) **26** (5 μM), and (f) **26** (10 μM). (E) The population in the S phase. (F) The population in the sub-G1 phase.

that exposure of exponentially growing HT-29 cells to **26** induced time-dependent apoptosis and growth inhibition and that the mechanism of **26**'s toxicity in mammalian cells was distinct from that of **1**.

The effect of **26** on induction of apoptosis was also evaluated by cell morphology (Figure 8A) and fluorescence-activated cell sorting (Figure 8B). Visual assessment of the immunostaining suggested that the majority of SKOV-3 and HT-29 cells were severely distorted or elongated and displayed membrane blebbing and cell shrinkage, and some cells turned round within 24 h after treatment with **26** (0.25 and 5 μg/mL), whereas the untreated control group displayed a normal shape and well-ordered cytoskeleton under the same conditions. Additionally, flow cytometry with the fluorescein isothiocyanate Annexin V/propidium iodide (PI) double staining assay was carried out to evaluate whether **26**-induced cell death was due to apoptosis or necrosis. The percentage of apoptotic cells (Annexin V^+/PI^- staining) in the control group was 4.5% for SKOV-3 cells and 20.7% for HT-29 cells (Figure 8B−D). After treatment with 5 and

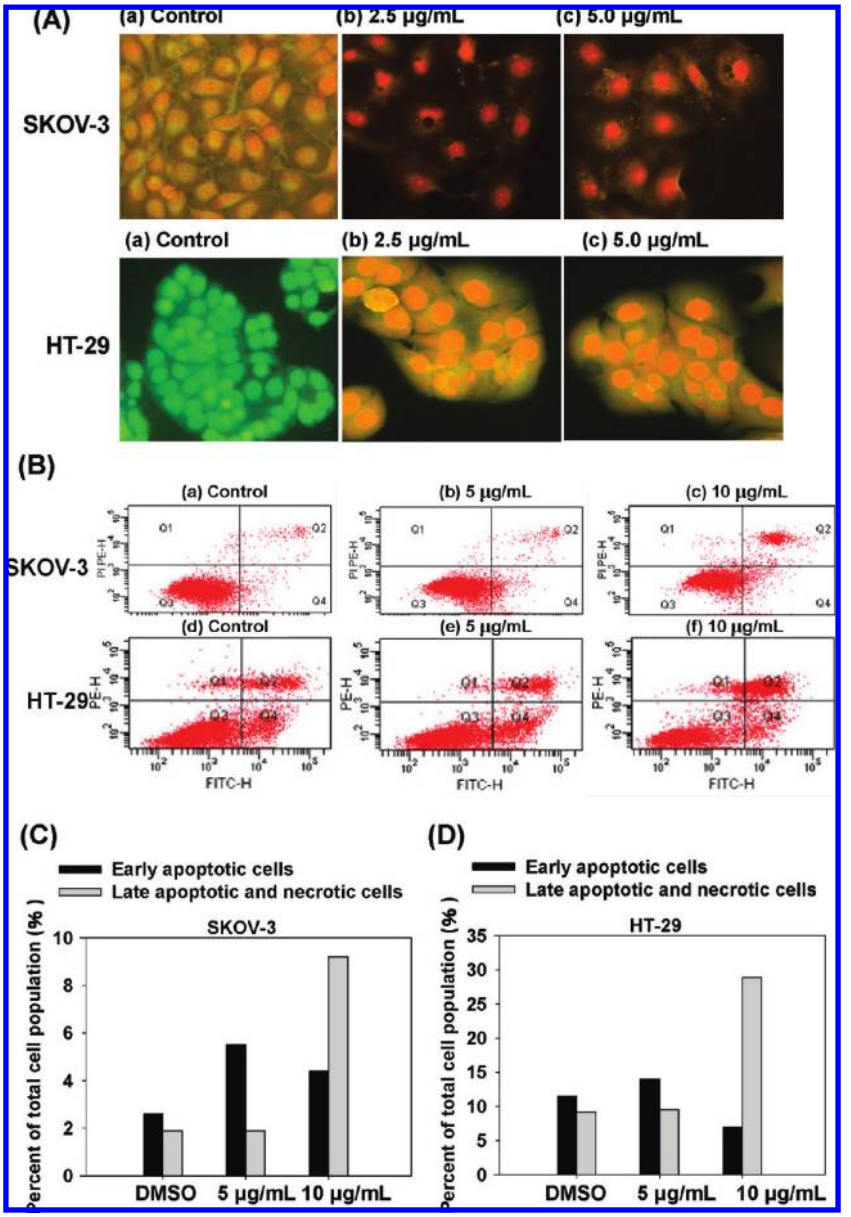

Figure 8. Compound **26** induces apoptosis of SKOV-3 and HT-29 cells. (A) Morphological changes of SKOV-3 (a−c) and HT-29 (d−f) cells after treatment with 2.5 or 5.0 μg/mL of **26**. (B) Compound **26** mediates SKOV-3 (a−c) and HT-29 (d−f) cell death. SKOV-3 and HT-29 cells were incubated in vitro without or with 5 or 10 μg/mL of **26** for 24 h and analyzed by Annexin V/PI cell viability assay. (C, D) Apoptotic (lower right quadrant) and necrotic (upper right quadrant) cells were identified and expressed as a percentage of total dead cells.

10 μg/mL of **26** for 24 h, the percentage of apoptotic cells increased to 7.4 and 13.6%, respectively, in the SKOV-3 cell line and increased to 23.5 and 35.9%, respectively, in the HT-29 line (Figure 8B−D). This assessment correlated well with the above DNA distribution results showing that **26** reduced the diploid DNA content and correspondingly increased the hypodiploid DNA content in HT-29 cells. Taken together, these results demonstrated that **26** induced cell death mainly via apoptosis.

We next evaluated the possibility that the pro-apoptotic activity of **26** in HT-29 cells was attributable to a higher level of induced DNA damage and/or altered DNA repair. The potential of **26** to induce DNA strand breaks in HT-29 cells was assessed via Comet assay using the Top I poison **1** as a positive control. At a concentration of 10 μM for 1 h, **26** caused a significant increase in DNA strand breaks (48%) as compared with untreated cells (9%); the percentage was 84% for **1**-treated cells (Figure 9A,B).

It is generally agreed that S phase arrest was a common hallmark of the death induced by DNA−Top I inhibitors. Taking all data above together, this novel lactone-free compound **26** induced DNA damage and apoptosis despite no alteration of cell cycle progression. According to the data from Top I-mediated cleavage and DNA distribution on HT 29 cell lines, it appeared that **26** trapped Top I−DNA covalent complexes with a potency and sequence selectivity different to that of **1**. Because it was previously reported that certain quinolone compounds possessed inhibitory activity against Top II,[16] we subsequently evaluated the effects of **26** against purified calf thymus Top II by relaxation of pRYG DNA according to the literature.[17] However, no inhibitory effect of **26** on Top II at 200 μM was observed (data not shown). Therefore, we speculated that an antitumor effect of **26** might be only partially dependent on Top I, indicating that **26** had additional targets besides Top I.

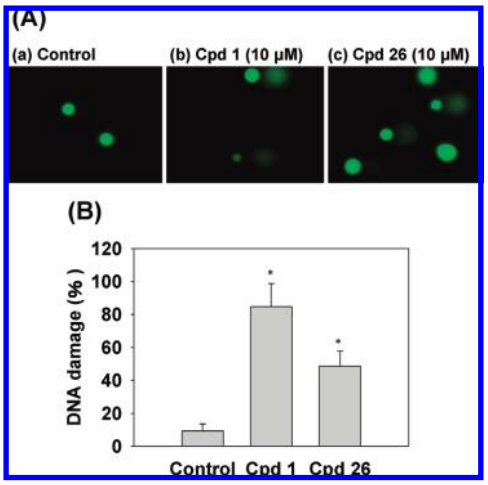

Figure 9. Compound **26** induces chromosomal DNA strand breaks as revealed by Comet assay. HT-29 cells were treated with **1** or **26** for 1 h. After treatment, the Comet assay was performed to assess chromosomal DNA integrity. (A) Comet images are representative of duplicates in three independent experiments. (B) Statistical significance was determined using Student's *t* test as compared with placebo control ($*P < 0.05$).

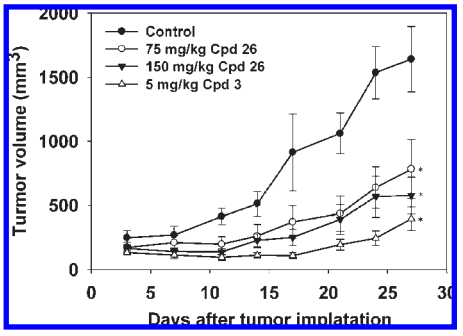

Figure 10. Effect of **26** on the growth of HT-29 tumor xenografts in nude mice. Nude mice bearing HT-29 tumor xenografts were treated daily with placebo (control) (●), **3** (positive control) at 5 mg/day/kg (△), **26** at 75 mg/day/kg (○), or 150 mg/day/kg (▼). The mean tumor volume was calculated by dividing the volume at each time point by the average volume of the tumors at the time when the treatment began. Data are expressed as means ± SEM of six samples from two experiments. Statistical significance was determined using Student's *t* test as compared with placebo control ($*P < 0.05$).

Compound 26 Inhibits the Growth of HT-29 Tumor Xenografts in Nude Mice. We next investigated the in vivo effect of **26** on the growth of HT-29 tumor xenografts. All 24 nude mice receiving a subcutaneous injection of HT-29 cells showed growth of solid tumors. As shown in Figure 10, the size of HT-29 tumor xenografts treated with the placebo increased steadily over time. Treatment with **3** at 5 mg/day/kg body weight, however, suppressed tumor growth by 76% as compared with placebo-treated controls. For **26**, tumor growth was suppressed by 52% (75 mg/day/kg group) or 65% (150 mg/day/kg group). Because of heterogeneity in tumor size, there was significant variation among the tumor volumes in each group, but the suppressive effect of **26** on tumor growth was clear when the representative tumors from the placebo and treated groups were compared side by side. None of the mice treated with **26** showed signs of morbidity or a change in body weight.

Conclusion

In summary, a novel series of Top I inhibitors were constructed by using a scaffold modification strategy: The rigid framework of **1** was changed into a combination of the quinolone skeleton and benzimidazole group or its bioisoesters through a single carbon bond. Thirty-one new compounds were synthesized and evaluated for anticell proliferation activity. The most potent compound **26** presented significant inhibitory effects on Top I and influences on Top I protein expression at the cellular level; moreover, **26** was proved to induce cell death via apoptosis rather than necrosis. Interestingly, further investigations of **26** to Top I-mediated cleavage and DNA distribution on tumor cell lines indicated that **26** trapped Top I cleavage complexes at different DNA sequences as compared with **1**. It could accelerate DNA strand breaks without significant alteration in cell cycle populations. Therefore, it was assumed that **26**'s cytotoxicity originated from both interacting with DNA−Top I complex and other mechanisms on the apoptotic pathway. Furthermore, the in vivo evaluation of **26** on the growth of HT-29 tumor xenografts in nude mice suggested its therapeutic potential for further development. Our scaffold modification approach based on **1** has yielded new generations of Top I inhibitors for cancer treatment. Further investigation on lead optimization and other molecular mechanisms are still under active investigation in our laboratories.

Experimental Section

General Experimental Procedures. Chemistry. All reagents were purchased from commercial sources and were used without further purification unless otherwise noted. Melting points (mp) were determined with a Mel-Temp II apparatus and are reported without any correction. Infrared spectra were obtained with Nicolet Impact 410 spectrophotometer using KBr film. The absorption band position is given in cm^{-1}. The ^1H NMR spectra were collected on a Bruker ACF-300 spectrometer (300 MHz) using Dimethyl sulfoxide (DMSO)-d_6 as the solvent with tetramethylsilane as the internal standard. Mass spectra were obtained on either a Mariner Mass Spectrum or a MAT-212 mass spectrometer. Elemental analyses were performed with a Carlo Erba 1106 elemental analysis apparatus. Each of the syntheses employed commercially available quinolone-3-carboxylic acids unless otherwise noted. Each of the target compounds was purified by silica gel (60 Å, 70−230 mesh) column chromatography. Concentration and evaporation of the solvent after reaction or extraction were carried out on a rotary evaporator (Buchi Rotavapor) operated at reduced pressure.

General Procedures for Compounds 6−20. A mixture of quinolone-3-carboxylic acids (0.1 mol) and *o*-phenylenediamine (0.01 mol), *o*-aminophenol (0.01 mol), or *o*-aminobenzenethiol (0.01 mol) in PPA (35 mL) was maintained at 130−140 °C to form a homogeneous phase. Each mixture was stirred at 170−250 °C for 4 h. After it was cooled to 100 °C, each mixture was poured slowly into 350 g of smashed ice with vigorous stirring. The pH of each solution was adjusted to neutral with 2.5 M NaOH. Each resulting solid was collected and purified by silica gel column chromatography (eluent, methanol:EtOAc = 1:2−1:4). The desired fraction in each case was collected, and the solvent was evaporated in vacuo. Each solid was recrystallized from methanol.

1-Ethyl-3-(benzimidazol-2-yl)-6-fluoro-7-(piperazin-1-yl)-4(1*H*)-quinolone (6). Compound **6** was obtained in 23.4% yield, mp 263 °C. IR (film): 3923 (NH), 2947, 1630 (CO), 1563, 1542, 1527, 1492, 1255, 879 cm^{-1}. ^1H NMR (DMSO-d_6): δ 1.44 (t, $J = 7.0$ Hz, 3 H, CH_3), 2.91 (m, 4 H, 2 × CH_2), 3.17 (m, 4 H, 2 × CH_2), 4.57 (q, $J = 7.0$ Hz, 2 H, CH_2), 7.13 (m, 3 H, 8-H and 5′-H and

6′-H), 7.61 (m, 2 H, 4′-H and 7′-H), 7.95 (d, J = 13.5 Hz, 1 H, 5-H), 9.17 (s, 1 H, 2-H), 12.69 (s, 1 H, 1′-H). ESIMS m/z (relative intensity) 391 (M^+), 349 (100), 306. Anal. ($C_{22}H_{22}FN_5O$) C, H, N. Calcd: 67.50, 5.66, 17.89. Found: 67.23, 5.77, 17.79.

1-Ethyl-3-(benzimidazol-2-yl)-6-fluoro-7-(1-piperazin-1-yl)-1,8-naphthyridine-4(1*H*)-one (7). Compound **7** was obtained in 18.9% yield, mp 225 °C. IR (film): 3488 (NH), 3058, 2979, 1634 (CO), 1474, 1445, 1257, 1139, 793, 738, 567 cm^{-1}. ^1H NMR (DMSO-d_6): δ 1.42 (t, J = 6.8 Hz, 3 H, CH_3), 2.98 (m, 4 H, 2 × CH_2), 3.90 (m, 4 H, 2 × CH_2), 4.51 (q, J = 6.8 Hz, 2 H, CH_2), 7.14 (m, 2 H, 5′-H and 6′-H), 7.61 (m, 2 H, 4′-H and 7′-H), 8.13 (d, J = 13.4 Hz, 2 H, 4′-H and 7′-H), 9.17 (s, 1 H, 2-H). ESIMS m/z (relative intensity). 392 (100, M^+). Anal. ($C_{21}H_{21}FN_6O$) C, H, N. Calcd: 64.27, 5.39, 21.41. Found: 64.39, 5.55, 21.13.

1-Ethyl-3-(benzimidazol-2-yl)-6,8-difluoro-7-(3-methylpiperazin-1-yl)-4(1*H*)-quinolone (8). Compound **8** was obtained in 14.2% yield, mp 272−275 °C. IR (film): 3313 (NH), 3057, 2980, 2936, 2736, 1626 (CO), 1574, 1544, 1527, 1477, 1385, 1282, 1250, 1143, 1051, 924, 790 cm^{-1}. ^1H NMR (DMSO-d_6): δ 1.19 (d, J = 6.8 Hz, 3 H, CH_3), 1.46 (t, J = 6.6 Hz, 3 H, CH_3), 3.13 (m, 4 H, 2 × CH_2), 3.39 (m, 3 H, CH_2, CH), 4.57 (q, J = 6.6 Hz, 2 H, CH_2), 7.14 (m, 2 H, 5′ -H and 6′-H), 7.61 (m, 2 H, 4′-H and 7′-H), 7.88 (d, J = 11.9 Hz, 1 H, 5-H), 9.08 (s, 1 H, 2-H), 12.59 (br, 1 H, NH). ESIMS m/z (relative intensity) 424 (100, MH^+). Anal. ($C_{23}H_{24}F_2N_5O$) C, H, N. Calcd: 65.24, 5.47, 8.97. Found: 65.35, 5.59, 8.85.

1-Ethyl-3-(benzimidazol-2-yl)-6-fluoro-7-(4-methylpiperazin-1-yl)-4(1*H*)- quinolone (9). Compound **9** was obtained in 26.4% yield, mp 239−242 °C (dec.). IR (film): 3329 (NH), 2925, 1620-(CO), 1550, 1473, 1284, 789 cm^{-1}. ^1H NMR(DMSO-d_6): δ 1.44 (t, 3H, $-CH_3$), 2.25 (s, 3H, $-CH_3$), 2.50 (m, 4H, 2 × CH_2), 3.27 (m, 4H, 2 × CH_2), 4.56 (q, 2H, CH_2), 7.12 (m, 3H, 8-H, 5′-H, 6′-H), 7.61 (m, 2H, 4′-H and 7′-H), 7.95 (d, 1H, 5-H), 9.17 (s, 1H, 1-H), 12.67 (s, 1H, 1′-H). EI-MS m/z 405 (M^+). Anal. ($C_{23}H_{24}FN_5O\cdot 2H_2O$) Calcd: 62.57, 6.34, 15.86. Found: 62.02, 6.13, 16.26. HR-MS: Found, 405.197192; Required, 405.196474; error, 0.718.

1-Ethyl-3-(benzoxazol-2-yl)-6-fluoro-7-chloro-4(1*H*)-quinolone (10). Compound **10** was obtained in 31.6% yield, mp 290 °C. IR (film): 1651 (CO), 1612, 1487, 1262, 1018, 749 cm^{-1}. ^1H NMR (DMSO-d_6): δ 1.41 (t, J = 7.1 Hz, 3 H, CH_3), 4.54 (q, J = 7.1 Hz, 2 H, CH_2), 7.38 (m, 2 H, 5′-H and 6′-H), 7.73 (m, 2 H, 4′-H and 7′-H), 8.13 (d, J = 9.1 Hz, 1H, 5-H), 8.27 (d, J = 6.6 Hz, 1 H, 8-H), 9.05 (s, 1 H, 2-H). ESIMS m/z (relative intensity) 342 (100, M^+), 314. Anal. ($C_{18}H_{12}ClFN_2O_2$) C, H, N. Calcd: 63.08, 3.53, 8.17. Found: 63.27, 3.61, 8.06.

1-Ethyl-3-(benzoxazol-2-yl)-6,8-difluoro-7-(3-methylpiperazin-1-yl)-4(1*H*)-quinolone (11). Compound **11** was obtained in 32.0% yield, mp 257 °C. IR (film): 3468 (NH), 2929, 1646 (CO), 1623, 1477, 1238, 1053, 1014, 833, 788 cm^{-1}. ^1H NMR (ppm, DMSO-d_6): δ 0.99 (d, J = 5.5 Hz, 3 H, CH_3), 1.44 (t, J = 6.7 Hz, 3 H, CH_3), 2.79−2.94 (m, 4 H, 2 × CH_2), 3.13 (m, 1 H, CH), 3.30 (m, 2 H, CH_2), 4.52 (q, 2 H, CH_2), 7.38 (q, 2 H, 5′-H and 6′-H), 7.74 (m, 2 H, 4′-H and 7′-H), 7.80 (d, J = 12.5 Hz, 1 H, 5-H), 8.91 (s, 1 H, 2-H). ESIMS m/z (relative intensity) 424 (M^+), 368 (100). Anal. ($C_{23}H_{22}F_2N_4O_2$) C, H, N. Calcd: 65.09, 5.22, 13.20. Found: 65.20, 5.34, 12.35.

1-Ethyl-3-(benzoxazol-2-yl)-6-fluoro-7-(4-methylpiperazin-1-yl)-4(1*H*)-quinolone (12). Compound **12** was obtained in 28% yield, mp 263 °C. IR (film): 2930, 1626 (CO), 1487, 1450, 1376, 1255, 1145, 1012, 742 cm^{-1}. ^1H NMR (DMSO-d_6): δ 1.43 (t, J = 7.0 Hz, 3 H, CH_3), 2.25 (s, 3 H, CH_3), 2.50 (m, 4 H, 2 × CH_2), 3.27 (m, 4 H, 2 × CH_2), 4.51 (q, J = 7.0 Hz, 2 H, CH_2), 7.10 (d, J = 7.3 Hz, 1 H, 8-H), 7.37 (m, 2 H, 5′-H and 6′-H), 7.72 (m, 2 H, 4′-H and 7′-H), 7.87 (d, J = 13.6 Hz, 1 H, 5-H), 8.94 (s, 1H, 1-H). ESIMS m/z (relative intensity) 406 (100, M^+). Anal. ($C_{23}H_{23}FN_4O_2\cdot 0.5H_2O$) C, H, N. Calcd: 66.49, 5.82, 13.48. Found: 66.31, 5.72, 13.60.

1-Ethyl-3-(benzoxazol-2-yl)-6-fluoro-7-(piperazin-1-yl)-1,8-naphthyridine-4(1*H*)-one (13). Compound **13** was obtained in 28.9% yield, mp 261 °C. IR (film): 3412 (NH), 3289, 2981, 1637 (CO), 1473, 1445, 1265, 792 cm^{-1}. ^1H NMR (DMSO-d_6): δ 1.40 (t, J = 7.0 Hz, 3 H, CH_3), 2.85 (m, 4 H, 2 × CH_2), 3.67 (m, 4 H, 2 × CH_2), 4.41 (q, J = 7.0 Hz, 2 H, CH_2), 7.37 (m, 2 H, 5′-H and 6′-H), 7.71 (m, 2 H, 4′-H and 7′-H), 7.98 (d, J = 13.7 Hz, 1 H, 5-H,), 8.93 (s, 1 H, 2-H). ESIMS m/z (relative intensity) 393 (M^+), 351 (100). Anal. ($C_{21}H_{20}F\ N_5O_2$) C, H, N. Calcd: 64.11, 5.12, 17.80. Found: 63.76, 5.34, 17.97.

1-Ethyl-3-(benzothiazol-2-yl)-6-fluoro-7-(piperazin-1-yl)-4(1*H*)-quinolone (14). Compound **14** was obtained in 22% yield, mp 290−295 °C. IR (film): 3429 (NH), 2938, 1615 (CO), 1493, 1254, 1010, 759 cm^{-1}. ^1H NMR (DMSO-d_6): δ 1.46 (t, J = 6.8 Hz, 3 H, $-CH_3$), 3.08 (m, 4 H, 2 × CH_2), 3.35 (m, 4H, 2 × CH_2), 4.62 (q, J = 6.8 Hz, 2 H, CH_2), 7.15 (d, J = 7.6 Hz, 1 H, 8-H), 7.38 (m, 1 H, 5′-H), 7.49 (m, 1 H, 6′-H), 7.95 (m, 2 H, 5-H and 7′-H), 8.09 (d, J = 7.6 Hz, 1 H, 4′-H), 9.23 (s, 1 H, 2-H). ESIMS m/z (relative intensity) 408 (M^+), 366 (100). Anal. ($C_{22}H_{21}FN_4OS$) C, H, N. Calcd: 64.69, 5.18, 13.72. Found: 64.55, 5.10, 13.70.

1-Ethyl-3-(benzothiazol-2-yl)-6-fluoro-7-(piperazin-1-yl)-1,8-naphthyridine-4(1*H*)-one (15). Compound **15** was obtained in 26.6% yield, mp 259−262 °C. IR (film): 3419 (NH), 1627 (CO), 1474, 1446, 1372, 1276, 792 cm^{-1}. ^1H NMR (DMSO-d_6): δ 1.44 (t, J = 6.8 Hz, 3 H, CH_3), 2.87 (m, 4 H, 2 × CH_2), 3.71 (m, 4 H, 2 × CH_2), 4.53 (q, J = 6.8 Hz, 2 H, CH_2), 7.37 (m, 1 H, 5′-H), 7.50 (m, 1 H, 6′-H), 7.96 (d, J = 8.0 Hz, 1 H, 7′-H), 8.07 (m, 2 H, 5-H and 4′-H), 9.24 (s, 1 H, 2-H). ESIMS m/z (relative intensity) 409 (M^+), 367 (100). Anal. ($C_{21}H_{20}FN_5OS\cdot H_2O$) C, H, N. Calcd: 59.00, 5.15, 16.38. Found: 58.88, 4.97, 16.26.

1-Ethyl-3-(benzothiazol-2-yl)-6-fluoro-7-(4-methylpiperazin-1-yl)-4(1*H*)-quinolone (16). Compound **16** was obtained in 25.7% yield, mp 226 °C. IR (film): 2931, 1617 (CO), 1570, 1497, 1452, 1259, 1009, 758 cm^{-1}. ^1H NMR (DMSO-d_6): δ 1.47 (t, J = 7.0 Hz, 3 H, $-CH_3$), 2.28 (s, 3 H, CH_3), 2.54 (m, 4 H, 2 × CH_2), 3.33 (m, 4 H, 2 × CH_2), 4.61 (q, J = 7.0 Hz, 2 H, CH_2), 7.16 (d, J = 7.2 Hz, 1 H, 8-H), 7.37 (t, J = 7.8 Hz, 1 H, 5′-H), 7.50 (t, J = 7.8 Hz, 1 H, 6′-H), 7.92−7.97 (m, 2 H, 5-H and 7′-H), 8.10 (d, J = 7.8 Hz, 1 H, 4′-H), 9.24 (s, 1 H, 1-H). ESIMS m/z (relative intensity) 422 (100, M^+), 323. Anal. ($C_{23}H_{23}FN_4OS\cdot 0.5H_2O$) C, H, N. Calcd: 64.02, 5.61, 12.98. Found: 63.83, 5.43, 13.25.

(*S*)-6-(Benzothiazol-2-yl)-9-fluoro-2,3-dihydro-3-methyl-10-(4-methylpiperazin-1-yl)-7-oxo-7*H*-pyrido[1,2,3-de][1,4]-benzoxazine (17). Levofloxacin (8 g, 0.02 mol), *o*-aminobenzenethiol (2.9 g, 0.02 mol), and PPA (90 mL) were used following the general procedure for the synthesis of **6**−**16**. Compound **17** was obtained in 50.9% yield, mp 259−262 °C. IR (film): 3010, 2976, 2924, 2797, 1611 (CO), 1585, 1547, 1479, 1468, 1452, 1296, 1236, 1133, 1046, 1011, 786, 760 cm^{-1}. ^1H NMR (DMSO-d_6): δ 1.49 (d, J = 7.0 Hz, 1 H, CH_3), 2.25 (s, 3 H, CH_3), 2.46 (m, 4 H, 2 × CH_2), 3.28 (m, 4 H, 2 × CH_2), 4.40 (m, 1 H, NCH), 4.60 (m, 1 H, OCH), 4.97 (m, 1 H, OCH), 7.38 (m, J = 7.6 Hz, 1 H, 5′-H), 7.50 (m, J = 7.0 Hz, 1 H, 6′-H), 7.58 (d, J = 12.5 Hz, 1 H, 8′-H), 7.95 (d, J = 7.8 Hz, 1 H, 7′-H), 8.10 (d, J = 7.8 Hz, 1 H, 4′-H), 9.22 (s, 1 H, 2-H). ESIMS m/z (relative intensity) 450 (100, M^+). Anal. ($C_{24}H_{23}FN_4O_2S\cdot H_2O$) C, H, N. Calcd: 61.52, 5.38, 11.96. Found: 61.29, 5.15, 11.85.

1-Ethyl-3-(benzothiazol-2-yl)-6,8-difluoro-7-(3-methylpiperazin-1-yl)-4(1*H*)-quinolone (18). Compound **18** was obtained in 15% yield, mp 224−227 °C. IR (film): 3428 (NH), 2956, 1611 (CO), 1491, 1323, 1054, 755 cm^{-1}. ^1H NMR (DMSO-d_6): δ 0.99 (d, J = 5.5 Hz, 3 H, CH_3), 1.44 (t, J = 7.0 Hz, 3 H, CH_3), 2.80−2.91 (m, 4 H, 2 × CH_2), 3.24−3.33 (m, 3 H, CH and CH_2), 4.59 (q, J = 7.0 Hz, 2 H, CH_2), 7.39 (t, J = 7.7 Hz, 1 H, 5′-H), 7.50 (t, J = 7.7 Hz, 1 H, 6′-H), 7.83 (d, J = 7.0 Hz, J = 10.9 Hz, 1 H, 5-H), 7.90 (d, J = 7.9 Hz, 1 H, 7′-H), 8.11 (d, J = 7.6 Hz, 1 H, 4′-H), 9.16 (s, 1 H, 2-H). ESIMS m/z (relative intensity) 440 (M^+), 384 (100). Anal. ($C_{23}H_{22}F_2N_4OS\cdot H_2O$) C, H, N. Calcd: 60.25, 5.28, 12.22. Found: 60.30, 5.06, 11.94.

1-Ethyl-3-(6-chlorobenzimidazol-2-yl)-6-fluoro-7-(piperazin-1-yl)-1,8-naphthyridine-4(1*H*)-one (18). Enoxacin (8 g, 0.025

mol), 4-chloro-1, 2-phenyldiamine (2.7 g, 0.025 mol), and PPA (90 mL) were used following the general procedure for the synthesis of **3**−**12**. Compound **18** was obtained in 18.1% yield, mp 261−264 °C. IR (film): 3408 (NH), 3067, 2982, 2867, 2462, 1632 (CO), 1565, 1525, 1477, 1446, 1275, 1256, 1141, 1055, 921, 794 cm^{-1}. ^1H NMR (DMSO-d_6): δ 1.41 (t, J = 7.0 Hz, 3 H, CH_3), 2.97 (m, 4 H, 2 × CH_2), 3.78 (m, 4 H, 2 × CH_2), 4.47 (q, J = 7.0 Hz, 2 H, CH_2), 7.16 (d, J = 8.1 Hz, 1 H, 4′-H), 7.61 (m, 2 H, 5′-H, 7′-H), 8.03 (d, J = 13.7 Hz, 1 H, 5-H), 9.11 (s, 1 H, 2-H), 12.79 (br, 1 H, NH). ESIMS m/z (relative intensity) 427 (100, MH^+). Anal. ($C_{21}H_{20}N_6OFCl$) C, H, N. Anal. ($C_{21}H_{20}ClFN_6O$) C, H, N. Calcd: 59.09, 4.72, 19.69. Found: 59.10, 4.80, 19.74.

1-Ethyl-3-(6-chlorobenzimidazol-2-yl)-6-fluoro-7-(piperazin-1-yl)-4(1*H*)-quinolone (20). Compound **20** was obtained in 21% yield, mp 261−262 °C. IR (film): 3422 (NH), 1629 (CO), 1492, 1255, 791 cm^{-1}. ^1H NMR (DMSO-d_6): δ 1.44 (t, J = 7.0 Hz, 3 H, $-CH_3$), 2.92 (m, 4 H, 2 × CH_2), 3.20(m, 4 H, 2 × CH_2), 4.57 (q, J = 7.0 Hz, J = 13.6 Hz, 2 H, CH_2), 7.13 (m, 2 H, 8-H and 4′-H), 7.56 (m, 1 H, 4′-H), 7.69 (m, 1 H, 5′-H), 7.94 (d, 1 H, 5-H), 9.14 (s, 1 H, 2-H), 12.84 (b, 1 H, 1′-H). ESIMS m/z (relative intensity) 425 (M^+), 383 (100). Anal. ($C_{22}H_{21}ClFN_5O\cdot 2H_2O$) C, H, N. Calcd: 57.20, 5.45, 15.16. Found: 56.97, 5.27, 15.27.

General Procedures for Compounds 21−33. 1-Ethyl-3-(6-nitrobenzimidazol-2-yl)-6-fluoro-7-(piperazin-1-yl)-4(1*H*)-quinolone (21). To a solution of **6** (0.8 g, 2.5 mmol) in concentrated sulfuric acid (3.20 mL) at 0 °C, concentrated nitric acid (0.26 mL, 3.7 mmol) was added dropwise with vigorous stirring. The internal temperature of the reaction flask was kept below 5 °C during the addition of nitric acid. After the addition of nitric acid, the solution was stirred at room temperature for 1 h and then at 35−40 °C for 2 h in a warm water bath. The solution was poured slowly into 350 g of smashed ice with vigorous stirring. The pH of the resulting solution was adjusted to 8 with 2.5 M NaOH. The precipitated solid was collected by suction filtration and purified by silica gel column chromatography (eluent, methanol:EtOAc = 1:6−1:8). The desired fraction was collected, and the solvent was evaporated in vacuo. The solid was recrystallized from methanol. Compound **21** was obtained in 33% yield, mp 236−240 °C. IR (film): 3414 (NH), 2978, 2841, 1628 (CO), 1568, 1524, 1493, 1451, 1385, 1311, 1269, 1191, 1140, 1057, 828 cm^{-1}. ^1H NMR (DMSO-d_6): δ 1.46 (t, J = 7.0 Hz, 3 H, CH_3), 3.07 (m, 4 H, 2 × CH_2), 3.17 (m, 4 H, 2 × CH_2), 4.59 (q, J = 7.0 Hz, 2 H, CH_2), 7.16 (s, 1 H, 8-H), 7.68, 7.84 (m, 1 H, 4′-H), 7.96 (d, J = 13.2 Hz, 1H, 5-H), 8.07 (m, 1 H, 5′-H), 8.38, 8.59 (m, 1 H, 7′-H), 9.22 (s, 1 H, 2-H), 13.23 (NH). ESIMS m/z (relative intensity) 436 (100, M^+). Anal. ($C_{22}H_{21}FN_6O_3$) C, H, N. Calcd: 60.54, 4.85, 19.26. Found: 60.37, 4.92, 19.10.

1-Ethyl-3-(6-nitrobenzimidazol-2-yl)-6-fluoro-7-(piperazin-1-yl)-1,8-naphthyridine-4(1*H*)-one (22). Following the synthetic procedure of **21**, **22** was obtained from **7** in 24% yield, mp 230−233 °C. IR (film): 3401 (NH), 3307 (NH), 2979, 1633 (CO), 1529, 1477, 1446, 1310, 1139, 795 cm^{-1}. ^1H NMR (DMSO-d_6): δ 1.42 (t, J = 7.0 Hz, 3 H, CH_3), 3.07 (m, 4 H, 2 × CH_2), 3.82 (m, 4 H, 2 × CH_2), 4.52 (q, J = 7.0 Hz, 2 H, CH_2), 7.69,7.82 (m, 1 H, 4′-H), 8.10 (m, 2 H, 5′-H and 5-H), 8.38, 8.59 (m, 1 H, 4′-H), 9.24 (s, 1 H, 2-H). ESIMS m/z (relative intensity) 437 (100, M^+), 395. Anal. ($C_{21}H_{20}N_7O_3F$) C, H, N. Calcd: 57.66, 4.61, 22.41. Found: 57.41, 4.78, 22.32.

1-Ethyl-3-(6-nitrobenzimidazol-2-yl)-6,8-difluoro-7-(3-methylpiperazin-1-yl)- 4(1*H*)-quinolone (23). Following the synthetic procedure of **21**, **23** was obtained from **8** in 27.1% yield, mp 269 °C (dec.). IR (film): 3420 (NH), 3069, 2982, 2937, 2853, 2733, 1622 (CO), 1580, 1526, 1477, 1389, 1333, 1249, 1143, 1089, 1053, 829, 736 cm^{-1}. ^1H NMR (DMSO-d_6): δ 1.06 (d, J = 6.8 Hz, 3 H, CH_3), 1.48 (t, J = 7.0 Hz, 3 H, CH_3), 3.16 3.33 (m, 7 H, 3 × CH_2, CH), 4.57 (q, J = 7.0 Hz, 2 H, CH_2), 7.65, 7.80 (m, 1 H, 4′-H), 7.84 (d, J = 11.7 Hz, 1H, 5-H), 8.03 (d, J = 8.0 Hz, 1H, 5-H), 8.42 (m, 1 H, 7′-H), 9.10 (s, 1 H, 2-H), 13.11 (br, 1 H, NH). ESIMS m/z (relative intensity) 469 (100, MH^+). Anal. ($C_{23}H_{23}F_2N_6O_3$) C, H, N. Calcd: 58.97, 4.73, 17.94. Found: 58.93, 4.86, 17.82.

1-Ethyl-3-(6-nitrobenzimidazol-2-yl)-6-fluoro-7-(4-methyl-1-piperazinyl)-4(1*H*)-quinolone (24). Compound **24** was obtained in 68% yield following the synthetic procedure described for **21**, mp 230−232 °C. IR (film): 3249 (NH), 2937, 1629 (CO), 1492, 1310, 1256, 1139, 1006, 790 cm^{-1}. ^1H NMR(DMSO-d_6): δ 1.45 (t, 3H, $-CH_3$), 3.06 (s, 3H, $-CH_3$), 2.58 (s, 4H, 2 × CH_2), 3.29 (s, 4H, 2 × CH_2), 4.59 (q, 2H, $-CH_2$), 7.10(d, 1H, 6′-H), 7.8 (dd, 1H, 7′-H), 7.93 (m, 1H, 5-H), 8.05 (m, 1H, 8-H), 8.78 (d, 1H, 4′-H), 9.18 (d, 1H, 2-H), 13.23 (s, 1H, 1′-H). EI-MS m/z 450 (M^+). HR-MS: ($C_{23}H_{23}FN_6O_3$) Found, 450.181602; Required, 450.181551; error, 0.101.

1-Ethyl-3-(6-nitrobenzoxazol-2-yl)-6-fluoro-7-chloro-4(1*H*)-quinolone (25). Following the synthetic procedure of **21**, **25** was obtained from **10** in 65.6% yield, mp 291−294 °C. IR (film): 3010, 2930, 1648 (CO), 1609, 1537, 1482, 1340, 1328, 1278, 1265, 1055, 1013, 827, 790, 760 cm^{-1}. ^1H NMR (DMSO-d_6): δ 1.43 (t, J = 7.0 Hz, 3 H, CH_3), 4.51 (q, J = 7.0 Hz, 2 H, CH_2), 7.80 (d, J = 7.0 Hz, 1 H, 4′-H), 8.00 (m, 1 H, 5′-H), 8.18 (m, 2 H, 5-H, 7′-H), 8.48 (s, 1 H, 8-H), 9.00 (s, 1 H, 2-H). ESIMS m/z (relative intensity) 388 (100, MH^+). Anal. ($C_{18}H_{11}ClFN_3O_4$) C, H, N. Calcd: 55.76, 2.86, 10.84. Found: 55.83, 2.96, 10.73.

1-Ethyl-3-(6-nitrobenzoxazol-2-yl)-6,8-difluoro-7-(3-methylpiperazin-1-yl)-4(1*H*)-quinolone (23). Following the synthetic procedure of **21**, **26** was obtained from **11** in 25.8% yield, mp 218 °C (dec.). IR (film): 3423 (NH), 3100, 3062, 2975, 2931, 2849, 2727, 1644, 1623 (CO), 1539, 1521, 1476, 1340, 1269, 1057, 827, 788, 734 cm^{-1}. ^1H NMR(DMSO-d_6): δ 1.06 (d, J = 7.0 Hz, 3 H, CH_3), 1.45 (t, J = 7.0 Hz, 3 H, CH_3), 2.90 (m, 4 H, 2 × CH_2), 3.46 (m, 3 H, CH_2 and CH), 4.53 (q, J = 7.0 Hz, 2 H, CH_2), 7.80 (d, J = 12.0 Hz, 1 H, 5-H), 7.91 (d, J = 8.7 Hz, 1 H, 4′-H), 8.27 (d, J = 8.7 Hz, 1 H, 5′-H), 8.62 (m, 1 H, 7′-H), 8.99 (s, 1 H, 2-H). ESIMS m/z (relative intensity) 470 (100, MH^+). Anal. ($C_{23}H_{21}F_2N_5O_4$) C, H, N. Calcd: 58.85, 4.51, 14.92. Found: 58.96, 4.42, 14.94.

1-Ethyl-3-(6-nitrobenzoxazol-2-yl)-6-fluoro-7-(4-methylpiperazin-1-yl)-4(1*H*)-quinolone (27). Following the synthetic procedure of **21**, **27** was obtained from **12** (2.0 g, 4.93 mmol) in 5.4% yield, mp 245−248 °C. IR (film): 3100, 3050, 2926, 1628 (CO), 1606, 1551, 1535, 1489, 1453, 1341, 1268, 1168, 1042, 998, 829, 790, 762 cm^{-1}. ^1H NMR (DMSO-d_6): δ 1.44 (t, J = 7.0 Hz, 3 H, CH_3), 2.26 (s, 3 H, NCH_3), 2.50 (m, 4 H, 2 × CH_2), 3.56 (m, 4 H, 2 × CH_2), 4.53 (q, J = 7.0 Hz, 2 H, CH_2), 7.08 (d, J = 7.4 Hz, 1 H, 8-H), 7.84 (m, 2-H, 5-H, 4′-H), 8.27 (d, J = 7.8 Hz, 1 H, 5′-H), 8.60 (d, J = 1.6 Hz, 1 H, 7′-H), 9.02 (s, 1 H, 2-H). ESIMS m/z (relative intensity) 452 (100, MH^+). Anal. ($C_{23}H_{22}FN_5O_4$) C, H, N. Calcd: 61.19, 4.91, 15.51. Found: 61.20, 4.71, 15.62.

1-Ethyl-3-(6-nitrobenzoxazol-2-yl)-6-fluoro-7-(piperazin-1-yl)-1,8-naphthyridine-4(1*H*)-one (28). Following the synthetic procedure of **21**, **28** was obtained from **13** in 17% yield, mp 258 °C (dec.). IR (film): 3411 (NH), 3099, 3059, 2983, 2934, 1632 (CO), 1606, 1584, 1540, 1477, 1446, 1383, 1341, 1271, 1233, 1163, 1128, 1091, 1054, 1003, 828, 794, 735 cm^{-1}. ^1H NMR (DMSO-d_6): δ 1.39 (t, J = 7.3 Hz, 3 H, CH_3), 3.00 (m, 4 H, 2 × CH_2), 3.75 (m, 4 H, 2 × CH_2), 4.42 (q, J = 7.3 Hz, 2 H, CH_2), 7.83 (d, J = 13.8 Hz, 1 H, 5-H), 8.21 (m, 2 H, 4′-H and 5′-H), 8.49 (s, 1 H, 7′-H), 8.98 (s, 1 H, 2-H). ESIMS m/z (relative intensity) 439 (100, MH^+). Anal. ($C_{21}H_{19}FN_6O_4$) C, H, N. Calcd: 57.53, 4.37, 19.17. Found: 57.62, 4.45, 19.08.

1-Ethyl-3-(6-nitrobenzothiazol-2-yl)-6-fluoro-7-(piperazin-1-yl)-4(1*H*)-quinolone (29). Following the synthetic procedure of **21**, **29** was obtained from **14** in 31.4% yield, mp 244 °C (dec.). IR (film): 3416 (NH), 3026, 2944, 2839, 1616 (CO), 1573, 1496, 1444, 1328, 1264, 1126, 894, 752 cm^{-1}. ^1H NMR (DMSO-d_6): δ 1.48 (t, J = 7.0 Hz, 3 H, CH_3), 3.08 (m, 4 H, 2 × CH_2), 3.32 (m, 4 H, 2 × CH_2), 4.61 (q, J = 7.0 Hz, 2 H, CH_2), 7.12 (d, J = 7.2 Hz, 1 H, 8-H), 7.88 (d, J = 13.3 Hz, 1 H, 5-H), 7.98 (d, J = 9.0 Hz, 1 H, 4′-H), 8.24 dd, J_1 = 9.0 Hz, J_2 = 2.4 Hz, 1 H, 5′-H), 9.08 (d, J = 2.4 Hz, 1 H, 7′-H), 9.24 (s, 1 H, 2-H). ESIMS m/z (relative

intensity) 454 (100, MH^+). Anal. ($C_{22}H_{21}FN_5O_3S$) C, H, N. Calcd: 53.27, 4.45, 15.44. Found: 53.38, 4.46, 15.29.

1-Ethyl-3-(6-nitrobenzothiazol-2-yl)-6-fluoro-7-(piperazin-1-yl)-1,8-naphthyridine-4(1*H*)-one (30). Following the synthetic procedure of **21**, **30** was obtained from **15** in 10.2% yield, mp 298 °C (dec.). IR (film): 3413 (NH), 3262, 3057, 2931, 2712, 1626 (CO), 1574, 1508, 1477, 1442, 1371, 1331, 1276, 1263, 1123, 792 cm^{-1}. ^1H NMR (DMSO-d_6): δ 1.46 (t, J = 7.0 Hz, 3 H, CH_3), 3.30 (m, 1 H, 2 × CH_2), 3.96 (m, 4 H, × CH_2), 4.57 (q, J = 7.0 Hz, 2 H, CH_2), 8.04 (d, J = 9.0 Hz, 1 H, 4′-H), 8.16 (d, J = 13.1 Hz, 1 H, 5-H), 8.30 (dd, J_1 = 9.0 Hz, J_2 = 2.6 Hz, 1 H, 5′-H), 9.14 (d, J = 2.6 Hz, 1 H, 7′-H), 9.35 (s, 1 H, 2-H). ESIMS m/z (relative intensity) 455 (100, MH^+). Anal. ($C_{21}H_{20}FN_6O_3S$) C, H, N. Calcd: 55.50, 4.21, 18.49. Found: 55.49, 4.19, 18.38.

1-Ethyl-3-(6-nitrobenzothiazol-2-yl)-6-fluoro-7-(4-methylpiperazin-1-yl)-4(1*H*)-quinolone (31). Following the synthetic procedure of **21**, **31** was obtained from **16** in 20.8% yield, mp 248 °C (dec.). IR (film): 3050, 2972, 2934, 2838, 1617 (CO), 1568, 1511, 1494, 1334, 1306, 1294, 1260, 1195, 1121, 1009, 896, 756 cm^{-1}. ^1H NMR (DMSO-d_6): δ 9.28 (s, 1 H, 2-H), 9.11 (s, J = 2.6 Hz, 1 H, 7′-H), 8.28 (dd, J_1 = 8.8 Hz, J_2 = 2.6 Hz, 1 H, 5′-H), 8.04 (d, J = 8.8 Hz, 1 H, 4′-H), 7.92 (d, J = 13.2 Hz, 1 H, 5-H), 7.14 (d, J = 7.7 Hz, 1 H, 8-H), 4.63 (q, J = 7.0 Hz, 2 H, CH_2), 3.71 (m, 4 H, 2 × CH_2), 2.63 (m, 4 H, 2 × CH_2), 2.34 (s, 3 H, CH_3), 1.40 (t, J = 7.0 Hz, 3 H, CH_3). ESIMS m/z (relative intensity) 468 (100, MH^+). Anal. ($C_{23}H_{23}FN_5O_3S$) C, H, N. Calcd: 59.09, 4.74, 14.98. Found: 59.16, 4.89, 14.83.

(*S*)-6-(6-Nitrobenzothiazol-2-yl)-9-fluoro-2,3-dihydro-3-methyl-10-(4-methylpiperazin-1-yl)-7-oxo-7*H*-pyrido[1,2,3-de][1,4]benzoxazine (32). Following the synthetic procedure of **21**, **32** was obtained from **17** in 17% yield, mp 266 °C. IR (film): 3100, 3010, 2973, 2931, 2840, 1614 (CO), 1573, 1513, 1476, 1440, 1332, 1294, 1235, 1126, 1047, 1006, 784, 753 cm^{-1}. ^1H NMR (DMSO-d_6): δ 1.51 (d, J = 6.5 Hz, 3 H, CH_3), 2.26 (s, 3 H, CH_3), 2.48 (m, 4 H, 2 × CH_2), 3.24 (m, 4 H, 2 × CH_2), 4.42 (m, 1 H, NCH), 4.60 (d, J = 10.8 Hz, 1 H, OCH), 4.99 (d, J = 10.8 Hz, 1 H, OCH), 7.54 (d, J = 12.6 Hz, 1 H, 5-H), 8.02 (d, J = 9.0 Hz, 1 H, 4′-H), 8.29 (dd, J_1 = 9.0 Hz, J_2 = 1.9 Hz, 1 H, 5′-H), 9.12 (d, J = 1.9 Hz, 1 H, 7′-H), 9.26 (s, 1 H, 2-H). ESIMS m/z (relative intensity) 496 (100, MH^+). Anal. ($C_{22}H_{23}FN_5O_4S$) C, H, N. Calcd: 58.17, 4.48, 14.13. Found: 58.27, 4.62, 14.22.

1-Ethyl-3-(6-nitrobenzothiazol-2-yl)-6,8-difluoro-7-(3-methylpiperazin-1-yl)-4(1*H*)-quinolone (33). Following the synthetic procedure of **21**, **33** was obtained from **18** in 14.6% yield, mp 217 °C (dec.). IR (film): 3418 (NH), 3081, 3055, 2981, 2841, 1609 (CO), 1546, 1509, 1482, 1381, 1333, 1250, 1124, 1056, 787, 753 cm^{-1}. ^1H NMR (DMSO-d_6): δ 1.04 (d, J = 7.1 Hz, 3 H, CH_3), 1.48 (t, J = 7.0 Hz, 3 H, CH_3), 2.78 (m, 4 H, 2 × CH_2), 3.03 (m, 3 H, CH_2, CH), 4.65 (q, J = 7.0 Hz, 2 H, CH_2), 7.88 (d, J = 13.2 Hz, 1 H, 5-H), 8.08 (d, J = 9.1 Hz, 1 H, 4′-H), 8.18 (dd, J_1 = 9.1 Hz, J_2 = 2.4 Hz, 1 H, 5′-H), 8.31 (d, J = 2.4 Hz, 1 H, 7′-H), 9.25 (s, 1 H, 2-H). ESIMS m/z (relative intensity) 486 (100, MH^+). Anal. calcd for ($C_{23}H_{22}F_2N_5O_3S$): C, 56.90; H, 4.36; N, 14.42. Found: C, 56.95; H, 4.49; N, 14.33.

General Procedure for Compounds 34−36. 1-Ethyl-3-(6-aminobenzoimidazol-2-yl)-6-fluoro-7-(piperazin-1-yl)-4(1*H*)-quinolone (34). To a solution of **21** (0.001 mol) in 1 N hydrochloric acid, 10% Pd/C was added with H_2 flow for 4 h. The mixture was filtered to 2.5 M NaOH. The precipitated solid was collected and dried to obtain **34** in 65.1% yield, mp 244−246 °C. IR (film): 3408 (NH), 3310, 3211, 2926, 2815, 2769, 2719, 2655, 2488, 1632 (CO), 1571, 1520, 1496, 1272, 1186, 1124, 1035, 828 cm^{-1}. ^1H NMR (DMSO-d_6): δ 1.50 (t, 3H, $-CH_3$), 2.51 (m, 4H, 2 × CH_2), 3.55 (m, 4H, 2 × CH_2), 4.55 (q, 2H, $-CH_2-$), 6.82 (dd, 1H, 5′-H), 6.99 (s, 1H, 8-H), 7.26 (d, 1H, 7′-H), 7.50 (d, 1H, 4′-H), 8.00 (d, 1H, 5-H), 9.36 (br), 9.46 (s, 1H, 2-H). HR-ESI-MS: ($C_{22}H_{24}FN_6O$) Found, 407.1991; Required, 407.1990; error, 0.1.

1-Ethyl-3-(5-aminobenzimidazol-2-yl)-6-fluoro-7-(4-methyl-1-piperazinyl)-4(1*H*)-quinolone (35). Compound **35** was obtained from **24** in 73.3% yield by an approach similar to that for **34**, mp 350 °C. IR (film): 3410 (NH), 3334, 1629 (CO), 1495, 1258, 1139, 790 cm^{-1}. ^1H NMR (DMSO-d_6):δ1.43 (t, 3H, $-CH_3$), 2.29 (s, 3H, $-CH_3$), 2.50(s, 2H, -NH_2), 2.57 (m, 4H, 2 × CH_2), 3.28 (m, 4H, 2 × CH_2), 4.55 (q, 2H, $-CH_2-$), 6.50 (s, 1H, 6′-H) 6.77 (s, 1H, 4′-H), 7.12 (d, 1H, 7′-H), 7.26 (d, 1H, 8-H), 7.94 (d, 1H, 5-H), 9.05 (s, 1H, 2-H). EI-MS m/z 420 (M^+). HR-MS: ($C_{23}H_{25}FN_6O$) Found, 420.207218; Required, 420.207372; error, 0.154.

1-Ethyl-3-(6-aminobenzoimidazol-2-yl)-6-fluoro-7-(piperazin-1-yl)-1,8-naph- thyridin-4(1*H*)-one (36). Compound **36** was obtained from **22** in 40.3% yield by an approach similar to that for **34**, mp 291 °C. IR (film): 3414 (NH), 3330, 3222, 3039, 2965, 2934, 2722, 1631 (CO), 1570, 1555, 1473, 1444, 1273, 792 cm^{-1}. ^1H NMR (DMSO-d_6): δ 1.44 (t, 3H, $-CH_3$), 3.33 (m, 4H, 2 × CH_2), 3.98 (m, 4H, 2 × CH_2), 4.52 (q, 2H, $-CH_2-$), 6.65 (dd, 1H, 5′-H), 6.87 (s, 1H, 7′-H), 7.36 (d, 1H, 4′-H), 8.17 (d, 1H, 5-H), 9.46 (s, 1H, 2-H). HR-ESI-MS (M + 1): ($C_{21}H_{23}FN_7O$) Found, 408.1938; Required, 408.1943; error, 0.5.

Materials and Methods for Biological Assay. Reagents. DMSO, **1**, SRB, and MTT were from Sigma Chemical Co. (St. Louis, MO). Top I and the plasmid pBR322 DNA were purchased from Takara-Bio (Shiga, Japan). All other reagents were of analytical grade or the highest grade available. Stock solutions of **1**, **3**, and all test compounds were dissolved in DMSO and stored at −20 °C.

Cell Lines and Cell Culture. Human cancer cell lines used in this study were obtained from the Culture Collection and Research Center (CCRC, Hsinchu, Taiwan) and cultured in the recommended media.

SRB Assay and Tetrazolium-Based MTT Assay for Cell Viability. The cytotoxicity of compounds was assessed by the MTT (for suspension cells)[18] and SRB (for adherent cells)[19,20] methods. Briefly, various cell lines were cultured at 5×10^3 cells per well containing 100 μL of culture medium (the seeding density depended on the doubling time of the different culture cell lines). After overnight incubation, the medium was discarded and then replaced with serum-free medium containing the desired concentrations (0, 0.08, 0.16, 0.32, 0.63, 1.25, 2.5, 5, and 10 μM) of test compounds dispensed from serial dilutions, and the plates were incubated for another 48 h at 37 °C. For SRB assay, the incubation was terminated by the addition of trichloroacetic acid (10% w/v final concentration in PBS), and then, SRB dye (0.4% w/v final concentration in 1% v/v acetic acid/H_2O) was added to stain the cells. Bound dye was subsequently dissolved with 10 mM Tris base (Sigma), and absorbance of the solution at 515 nm was determined using an Emax Microplate readers and SoftMax Pro software (Molecular Devices, United States). For MTT assay, cells were washed once before adding 50 μL of fetal bovine serum-free medium containing MTT (0.5 mg/mL final concentration in PBS). After 4 h of incubation at 37 °C, the medium was discarded, and the formazan blue that formed in the cells was dissolved in DMSO. The optical density was measured at 570 nm. The GI_{50} and IC_{50} values were estimated by plotting the colorimetric data on SigmaPlot 10.0 version (Systat Software Inc., United States), and the data were fitted to an exponential decay function to generate a common log concentration−response curve.

Anchorage-Dependent Growth. The anchorage-dependent colony-forming assay was used to evaluate the long-term growth inhibitory effect of **26**.[21] Briefly, HT-29 cells were seeded at a density of 500 cells/well in six-well plates, and after a 24 h attachment period, the cultures were continuously treated with the indicated concentrations of test compounds or DMSO for 14 days. Medium containing **1**, **3**, **26**, or DMSO was replaced every 72 h during the 14 day period. The cell colonies were then fixed in 1% (v/v) formaldehyde in phosphate-buffered saline (PBS) and stained with 0.1% (w/v) crystal violet in PBS (Sigma). Images were collected by single rapid scans (MicroTek ScanMaker 5900, China).

Top I Inhibition Assay. Top I activity was measured by the relaxation of superhelical DNA in plasmid pBR322.[22] Each 20 μL assay contained 50 mM Tris-HCl (pH 8.0), 120 mM KCl, 10 mM $MgCl_2$, 0.5 mM EDTA, 0.01% (w/v) bovine serum albumin, pBR322 DNA (0.5 μg), and test compounds at various concentrations (see the Results and Discussion) or vehicle alone (for controls). The reaction was started by the addition of 1 U of Top I and allowed to proceed at 37 °C for 30 min. Aliquots of 20 μL were subjected to electrophoresis in 1% agarose gel (Bio-Rad, United Kingdom) using Mupid-2 mini-Gel units (Cosmo Bio, Japan) at 100 V for 1 h in 0.5× Tris/acetate (TAE) buffer (20 mM Tris-acetate, 0.5 mM EDTA, pH 8.3). The gels were stained with 0.5 mg/mL ethidium bromide for 30 min and destained in distilled water for 10 min. The DNA bands were visualized by illumination from below with short-wave ultraviolet light and photographed. For quantitative determinations, the integrated intensity of the ethidium bromide fluorescence of the bands (relaxed form) was acquired and measured using BioDoc-IT Imaging System (UVP, Inc., CA). Plasmid pBR322 DNA alone (lane 1 in all gels) and pBR322 DNA relaxed by Top I (lane 2 in all gels) were taken as the negative and positive (100% activity) controls, respectively. DNA bands were quantified and calculated from gel photographs using ImageQuant image analysis software (GE Healthcare, United Kingdom) and SigmaPlot 10.0.

Top I-Mediated DNA Cleavage Reactions. Human recombinant Top I and pRYG plasmid were purchased from TopoGEN (Columbus, OH). The full length fragment of pRYG plasmid was cleaved with the restriction endonuclease *Hind* III (New England Biolabs, MA) in supplied NE buffer 2 (50 μL reactions) for 1 h at 37 °C and checked by electrophoresis in a 1% agarose gel made in 0.5× TAE buffer. Approximately 3 μg of the fragment was terminal end-labeled at the *Hind* III site by fill-in reaction with [α-^{32}P]dCTP, and 10 μM dATP and dGTP, in Klenow buffer (50 mM Tris, 5 mM $MgCl_2$, and 0.01% Triton X-100) with 5 units of Exofree Klenow fragment (Genemark Technology Co., Ltd., Taiwan). Unincorporated ^{32}P-dCTP was removed using Gel/PCR DNA Fragments Extraction Kit (Geneaid Biotech Ltd., Taiwan), and the eluate containing the terminal end-labeled fragment was collected and measured the specific activity of the labeled DNA by measuring 1 μL in a scintillation counter (Beckman LS 6000IC Liquid Scintillation Systems). Aliquots (approximately 100000 cpm/ reaction) were incubated with Top I in reaction buffer [40 mM Tris-HCl (pH 8.0), 100 mM KCl, 10 mM $MgCl_2$, 0.5 mM dithiothreitol, 0.5 mM EDTA, and 30 μg/mL bovine serum albumin] at 25 °C for 30 min in the presence of the tested compounds. Reactions were terminated by adding SDS (5% final concentration) and proteinase K (4 mg/mL final concentration) for further incubation at 45 °C for 30 min. Samples were then alkali-denatured by the addition of NaOH (0.15 N final concentration), mixed with loading buffer (80% formamide, 10 mM sodium hydroxide, 1 mM sodium EDTA, 0.1% xylene cyanol, and 0.1% bromophenol blue, pH 8.0), and analyzed by electrophoresis in 1% agarose gel in 0.5× TAE electrophoresis buffer. After electrophoresis, gels were dried onto Whatman 3MM chromatographic paper using a gel dryer (Bio-Rad Lab., Hercules, CA) at 80 °C for 1 h and autoradiographed at −80 °C using Kodak XAR-5 film.

Immunocytochemical Studies. Immunocytochemistry was used to detect Top I expression in cancer cell lines. Staining was performed according to the standard protocol for immunoperoxidase enzyme detection.[23] To inhibit peroxidase activity, slides were placed in freshly prepared 0.3% H_2O_2 in methanol for 10 min before blocking in PBS containing 10% normal goat serum. A primary antibody to Top I was applied for 10 h at a dilution of 1:100 in PBS. Secondary biotinylated antigoat IgG was then applied for 2 h at room temperature. The remaining steps of incubation involved avidin-biotinylated horseradish peroxidase solution for 2 h, then detection of immunoperoxidase activity by freshly prepared substrate (0.05%, 3,3′-diaminobenzidine tetrahydrochloride, DAB), counter staining, and mounting by dimethyl benzene. Cells were distinguished based on their immediate location along scalloped trabecular surfaces, multiple nuclei, enrichment of vacuoles in the basophilic cytoplasm, and a ruffled border appearance.

Flow Cytometry for DNA Content Analysis. HT-29 cells were treated with vehicle or the indicated concentrations of test compounds for the indicated times and then released by incubated with trypsin-EDTA. Both attached and floating cells were collected and fixed with 70% ethanol. Cells were then incubated for 30 min with 0.1% (v/v) Triton X-100, washed again, and subsequently stained with 50 μg/mL PI and 50 μg/mL RNaseA in PBS for 30 min in the dark at room temperature. For cell cycle analysis, 10000 cells were determined using flow cytometry on a BD FACSCalibur cytometer, and the data were analyzed by CellQuest software (Becton Dickinson, CA). The red fluorescence (FL2) of single events was recorded using an argon ion laser (488 nm excitation, 610 nm emission) to measure the DNA index. The percentage of apoptotic cells was calculated from the number of cells in sub-G1 phase, representing fragmented cell vesicles.

Immunostaining for Nuclei. All floating and attached cells were harvested with 0.02% (w/v) EDTA and 0.25% (w/v) trypsin. The cell suspension in RMPI 1640 medium containing 10% heated-inactivated calf serum was then added to bring the total volume of each well to 500 μL. Different concentrations of **26** were added after 24 h and incubated for an additional 48 h. The cell suspension was washed with PBS followed by the addition of 4% (w/v) formaldehyde in PBS and fixation for 20 min, and then, the mixture was washed with PBS. Hoechst 33342 (10 μg/mL) was added and retained for 5−10 min. The cell morphology was monitored under an inverted light microscope. The cells were then observed under a fluorescence microscope (Olympus IX51, Japan) with a peak excitation wavelength of 490 nm.

Annexin V/PI Double-Staining Assay. SKOV-3 and HT-29 cells (1−5 × 10^6 cells/mL) were treated with **26** for 24 h, harvested, and then washed and resuspended with PBS. Apoptotic cells were identified by double supravital staining with recombinant enhanced green fluorescent protein (EGFP)-conjugated Annexin V^+/PI^-, using the Annexin V-EGFP Apoptosis Detection kit (KeyGen, China) according to the manufacturer's instructions. Flow cytometric analysis was performed immediately after supravital staining. Data acquisition and analysis were performed with FACSCalibur and CellQuest software. Cells not binding EGFP-Annexin V and excluding PI were classified as Annexin V negative. Cells that bound EGFP-Annexin V [excitation wavelength (λ_{ex}) = 488 nm, emission wavelength (λ_{em}) = 520 nm] but excluded PI (λ_{ex} = 540 nm, λ_{em} = 630 nm) were termed Annexin V positive. Cells permeant to PI (regardless of whether they bound EGFP-Annexin V) were deemed necrotic.

Comet Assay for Top I-Cleavable Complexes. The Comet assay, or single-cell gel electrophoresis (SSGE), has been used extensively to monitor the integrity of chromosomal DNA and the amount of Top I-cleavable complexes; the assay was performed essentially as described.[24,25] Briefly, exponentially growing HT-29 cells were subcultured in 24-well plates at 1 × 10^4 cells/well and allowed to attach overnight. Negative control cells were not treated with **26**, whereas positive control cells for DNA strand breaks were treated with **1**. Cells were then treated with 10 μM **26** for 1 h. The first layer of agarose on microscope slides was prepared by dipping the slides into 1% normal-melting agarose followed by drying; separately, 50 μL of HT-29 cell suspension (1 × 10^4 cells) was mixed with 100 μL of 1.5% low-melting point agarose and then poured onto a fully frosted slide that had been precoated with 1% normal-melting agarose A coverslip was then applied to each slide. The slides were submerged in prechilled lysis solution (1% *N*-lauryl sarcosine, 1%

Triton X-100, 2.5 M NaCl, and 10 mM EDTA, pH 10.5) for 30 min at 4 °C. After lysing, the slides were drained and placed on a horizontal electrophoresis tray with freshly made alkaline buffer (300 mM NaOH and 1 mM EDTA; pH > 13) for 30 min at 4 °C to allow the DNA to unwind. After they were soaked with alkaline buffer, the slides were subjected to electrophoresis for 10 min at 16 V (25 mA) at room temperature. After electrophoresis, slides were stained with SyBr Gold (Molecular Probes, United States), and images of nuclei were captured with a Zeiss Axiophot 2 microscope (Carl Zeiss Inc., United States) connected to a Spot CCD camera and SPOT software (Diagnostic Instruments Inc., United States). DNA damage, reported as the mean percentage of DNA in the tail, was quantified in at least 50 randomly selected nuclei for each experimental point.

In Vivo Activity of 26 against Established Tumor Xenografts in Nude Mice. Female athymic BALB/c nude mice (35−40 days old) with body weights ranging from 18 to 22 g were supplied by the Beijing Institute of Materia Medica, Chinese Academy of Medical Sciences. Animal care and surgery protocols were approved by the Animal Care Committees of the China Pharmaceutical University. All animals were appropriately treated in a scientifically valid and ethical manner. For inoculation of nude mice, a suspension of 1×10^7 HT-29 cells in 200 μL of culture medium was subcutaneously transplanted into the axillary fossa of each BALB/c nude mouse. When the diameter of a resultant tumor reached ~1 mm, as measured with a vernier caliper, the tumor was excised and then sterilely and uniformly transplanted into the axillary fossa of a nude mouse (24 mice were used, total). Treatment was begun when implanted tumors had reached a volume of about 100−300 mm^3 (after 1 week, on average). Mice were randomized into four groups ($n = 6$ each) and treated daily by intraperitoneal injection with 400 μL of physiological saline for 10 days, **3** at 5 mg/kg body weight in 400 μL for 2 days, or **26** at 75 or 150 mg/kg body weight in 400 μL for 10 consecutive days. Tumor volumes were monitored by caliper measurement of the length and width and calculated using the formula of $V = 1/2 \times a \times b^2$, where a is the tumor length and b is the width. Tumor volumes and body weights were monitored every 4 days over the course of treatment. Mice were sacrificed on day 30 following initiation of treatment, and tumors were removed and recorded for analysis.

Statistical Analysis. SigmaStat 10.0 software was used for statistical analyses. Body weight and tumor growth were analyzed by the Student's t test to show significant differences between the test groups and the control groups. Probability values below 0.05 were considered significant.

Acknowledgment. This work was supported by Research Grants 30271543 and 30472084 to Q.-D.Y. from the National Natural Science Foundation (NSFC) of China and by a research grant to J.-W.C. from the National Science Council of Taiwan (NSC97-2323-B-002-010).

References

(1) Thomas, C. J.; Rahier, N. J.; Hecht, S. M. Camptothecin: Current perspectives. *Bioorg. Med. Chem.* **2004**, *12*, 1585–1604.
(2) Wall, M. E.; W., M. C.; Cook, C. E.; Palmar, K. H.; McPhail, A. T.; Sim, G. A. Plant antitumor agents. I. The isolation and structure of camptothecin, a novel alkaloidal leukemia and tumor inhibitor from *Camptotheca acuminata*. *J. Am. Chem. Soc.* **1966**, *88*, 3888–3890.
(3) Covey, J. M.; Jaxel, C.; Kohn, K. W.; Pommier, Y. Protein-linked DNA strand breaks induced in mammalian cells by camptothecin, an inhibitor of topoisomerase I. *Cancer Res.* **1989**, *49*, 5016–5022.
(4) Hertzberg, R. P.; Caranfa, M. J.; Hecht, S. M. On the mechanism of topoisomerase I inhibition by camptothecin: Evidence for binding to an enzyme-DNA complex. *Biochemistry* **1989**, *28*, 4629–4638.
(5) Giovanella, B. C.; Stehlin, J. S.; Wall, M. E.; Wani, M. C.; Nicholas, A. W.; Liu, L. F.; Silber, R.; Potmesil, M. DNA topoisomerase I—Targeted chemotherapy of human colon cancer in xenografts. *Science* **1989**, *246*, 1046–1048.
(6) Saltz, L. B.; Cox, J. V.; Blanke, C.; Rosen, L. S.; Fehrenbacher, L.; Moore, M. J.; Maroun, J. A.; Ackland, S. P.; Locker, P. K.; Pirotta, N.; Elfring, G. L.; Miller, L. L. Irinotecan plus fluorouracil and leucovorin for metastatic colorectal cancer. Irinotecan Study Group. *N. Engl. J. Med.* **2000**, *343*, 905–914.
(7) Fassberg, J.; Stella, V. J. A kinetic and mechanistic study of the hydrolysis of camptothecin and some analogues. *J. Pharm. Sci.* **1992**, *81*, 676–684.
(8) Fox, B. M.; Xiao, X.; Antony, S.; Kohlhagen, G.; Pommier, Y.; Staker, B. L.; Stewart, L.; Cushman, M. Design, synthesis, and biological evaluation of cytotoxic 11-alkenylindenoisoquinoline topoisomerase I inhibitors and indenoisoquinoline-camptothecin hybrids. *J. Med. Chem.* **2003**, *46*, 3275–3282.
(9) Morrell, A.; Antony, S.; Kohlhagen, G.; Pommier, Y.; Cushman, M. A systematic study of nitrated indenoisoquinolines reveals a potent topoisomerase I inhibitor. *J. Med. Chem.* **2006**, *49*, 7740–7753.
(10) Pommier, Y. Topoisomerase I inhibitors: camptothecins and beyond. *Nat. Rev. Cancer* **2006**, *6*, 789–802.
(11) Xiao, X.; Antony, S.; Pommier, Y.; Cushman, M. Total synthesis and biological evaluation of 22-hydroxyacuminatine. *J. Med. Chem.* **2006**, *49*, 1408–1412.
(12) Pommier, Y. DNA topoisomerase I inhibitors: Chemistry, biology, and interfacial inhibition. *Chem. Rev.* **2009**, *109*, 2894–2902.
(13) Mauser, H.; Guba, W. Recent developments in de novo design and scaffold hopping. *Curr. Opin. Drug Discovery Dev.* **2008**, *11*, 365–374.
(14) Horowitz, S.; Maor, R.; Priel, E. Characterization of DNA topoisomerase activity in two strains of *Mycoplasma fermentans* and in *Mycoplasma pirum*. *J. Bacteriol.* **1997**, *179*, 6626–6632.
(15) Holm, C.; Covey, J. M.; Kerrigan, D.; Pommier, Y. Differential requirement of DNA replication for the cytotoxicity of DNA topoisomerase I and II inhibitors in Chinese hamster DC3F cells. *Cancer Res.* **1989**, *49*, 6365–6368.
(16) Verma, R. P. Understanding topoisomerase I and II in terms of QSAR. *Bioorg. Med. Chem.* **2005**, *13*, 1059–1067.
(17) Yamashita, Y.; Kawada, S.; Fujii, N.; Nakano, H. Induction of mammalian DNA topoisomerase II dependent DNA cleavage by antitumor antibiotic streptonigrin. *Cancer Res.* **1990**, *50*, 5841–5844.
(18) Carmichael, J.; DeGraff, W. G.; Gazdar, A. F.; Minna, J. D.; Mitchell, J. B. Evaluation of a tetrazolium-based semiautomated colorimetric assay: Assessment of chemosensitivity testing. *Cancer Res.* **1987**, *47*, 936–942.
(19) Vichai, V.; Kirtikara, K.; Sulforhodamine, B. Colorimetric assay for cytotoxicity screening. *Nat. Protoc.* **2006**, *1*, 1112–1116.
(20) Voigt, W. Sulforhodamine B assay and chemosensitivity. *Methods Mol. Med.* **2005**, *110*, 39–48.
(21) Jinno, H.; Steiner, M. G.; Mehta, R. G.; Osborne, M. P.; Telang, N. T. Inhibition of aberrant proliferation and induction of apoptosis in HER-2/neu oncogene transformed human mammary epithelial cells by N-(4-hydroxyphenyl)retinamide. *Carcinogenesis* **1999**, *20*, 229–236.
(22) Topcu, Z.; Castora, F. J. Mammalian mitochondrial DNA topoisomerase I preferentially relaxes supercoils in plasmids containing specific mitochondrial DNA sequences. *Biochim. Biophys. Acta* **1995**, *1264*, 377–387.
(23) Feister, H. A.; Onyia, J. E.; Miles, R. R.; Yang, X.; Galvin, R.; Hock, J. M.; Bidwell, J. P. The expression of the nuclear matrix proteins NuMA, topoisomerase II-alpha, and -beta in bone and osseous cell culture: Regulation by parathyroid hormone. *Bone* **2000**, *26*, 227–234.
(24) Singh, N. P.; McCoy, M. T.; Tice, R. R.; Schneider, E. L. A simple technique for quantitation of low levels of DNA damage in individual cells. *Exp. Cell Res.* **1988**, *175*, 184–191.
(25) Tice, R. R.; Agurell, E.; Anderson, D.; Burlinson, B.; HartmannA.; Kobayashi, H.; Miyamae, Y.; Rojas, E.; Ryu, J. C.; Sasaki, Y. F. Single cell gel/comet assay: Guidelines for in vitro and in vivo genetic toxicology testing. *Environ. Mol. Mutagen.* **2000**, *35*, 206–221.